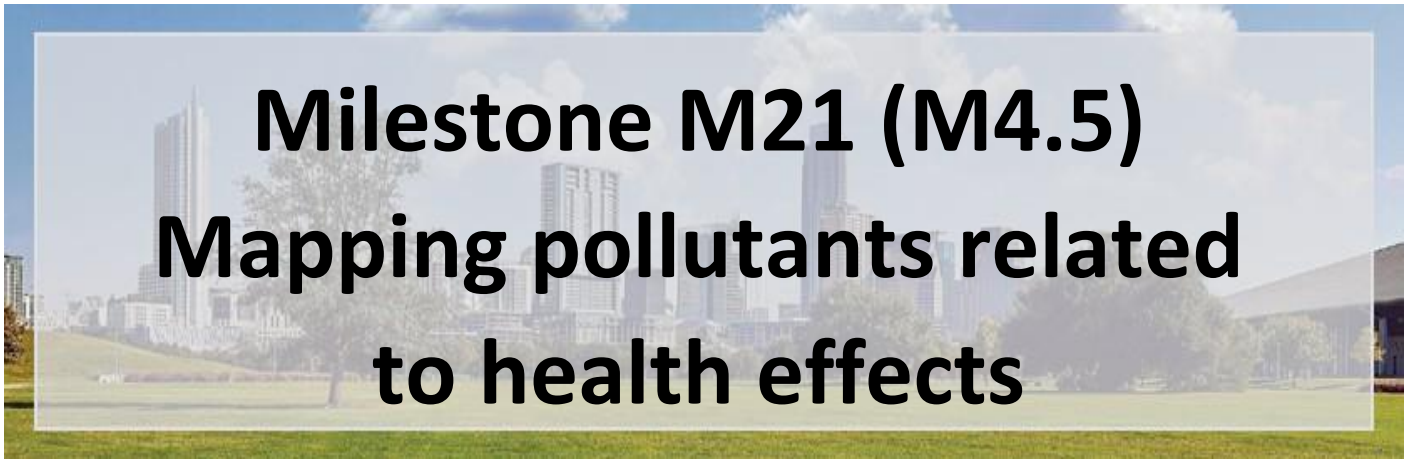

Milestone M21 (M4.5)
Mapping pollutants related to health effects

RI-URBANS

Research Infrastructures Services Reinforcing Air Quality Monitoring Capacities in European Urban & Industrial AreaS (GA n. 101036245)

By

CNRS, ENPC, UU, INOE, UoB, VITO & NOA

27th September 2023

RI-URBANS (www.RIURBANS.eu) is supported by the European Commission under the Horizon 2020 – Research and Innovation Framework Programme, H2020-GD-2020, Grant Agreement number: 101036245

Milestone M21 (M4.5): Mapping pollutants related to health effects

Authors: Karine Sartelet (CNRS/ENPC), Gerard Hoek (UU), Eleni Athanasopoulou (NOA), Dimitrios Bousiotis (UoB), Fabrice Dugay (Airparif), Roy Harrison (UoB) , Jelle Hofman (VITO), Alexandru Ilie (INOE), Jules Kerckhoffs (UU), Lya Lugon (CNRS/ENPC), Doina Nicolae (INOE), Soojin Park (CNRS/ENPC), Francis Pope (UoB), , Camelia Talianu (INOE), Myrto Valari (CNRS/LMD), Martine Vanpoppel (VITO), Jeni Vasilescu (INOE) & Jian Zhong (UoB)

Work package (WP)	WP4 Pilot implementations for testing and demonstrating services
Milestone	M21 (M4.5)
Lead beneficiary	CNRS
Means of verification	maps available on-line
Estimated delivery deadline	M24 (30/09/2023)
Actual delivery deadline	27/09/2020
Version	Final
Reviewed by	WP4 leaders and coordinators
Accepted by	Project Coordination Team
Comments	In this milestone, maps are produced using different approaches, and they are evaluated using fixed monitoring sites when possible. Further analysis is necessary to discuss the variability observed.

RI-URBANS (www.RIURBANS.eu) is supported by the European Commission under the Horizon 2020 – Research and Innovation Framework Programme, H2020-GD-2020, Grant Agreement number: 101036245

Table of Contents

RI-URBANS (www.RIURBANS.eu) is supported by the European Commission under the Horizon 2020 – Research and Innovation Framework Programme, H2020-GD-2020, Grant Agreement number: 101036245

1. About this document

Different techniques may be used to provide high-resolution outdoor exposure city maps for pollutants related to health effects, using modelling tools, mobile measurements of nanoparticles (=ultrafine particles, UFP), blac carbon (BC) and atmospheric particulate matter (PM) mid-cost sensors, novel dispersion measurements, and the participation of networks of citizens and new innovative instruments. In cities, sub-grid variability along traffic axes and streets is particularly important for nitrogen dioxide (NO_2), BC, organic matter (OM), number particle concentration (PNC=UFP) and $PM_{2.5}$ and PM_{10}. Maps are required at spatial scales below 100 m, at the minimum at the annual average scale but preferably at an hourly scale for summer and winter seasons.

In cities, the urban background concentrations are simulated with chemical transport models, which typically have horizontal resolutions coarser than 1 km x 1 km, and they cannot capture the city heterogeneities. Two approaches are used to represent these heterogeneities:

- Deterministic models with a multi-scale and multi-pollutant (NO_2, $PM_{2.5}$, PM_{10}, BC, organic aerosols (OA), PNC-UFP) approach (Paris, Birmingham and Athens), which can be corrected using data assimilation (Paris).
- Analysis of mobile monitoring and/or citizen observations using Land Use Regression (LUR) modelling (Rotterdam, Bucharest) or machine learning (Birmingham) to map PNC-UFP, $PM_{2.5}$, NO_2.

Evaluation of the validity of maps of modelled air pollutant concentrations across cities is challenging because of the generally spatially sparse monitoring data. The difficulty lies in evaluating the models at different types of stations characteristic of urban areas (traffic, urban background, suburban). This applies to regulated pollutants such as NO_2 and $PM_{2.5}$ in most cities, but even more for the non-regulated pollutants PNC-UFP and BC, for which routine monitoring is scarce. Therefore, it is difficult to evaluate the performance of models to assesses the spatial variability across cities. This issue applies both to deterministic models and empirical models based on mobile monitoring. We can evaluate however whether the models broadly represent the measurements at the few monitoring sites that are typically available in cities. For the empirical models based on (mobile) monitoring data, we can compare the measurements with co-located measurements at routine monitoring sites. For the deterministic models, the ability to represent variability depends on the representation of emission variability and the type of model used to represent dispersion and physico-chemical transformations of emissions in urban areas. Data assimilation may be used to improve the maps, but it is difficult to implement for non-regulated pollutants for which observations are scarce.

In this milestone, maps are produced using the different approaches listed above, and they are evaluated using fixed monitoring sites when possible. Further analysis is necessary to discuss the variability observed. The difference of variability between pollutants can be characterized using ratios of pollutant concentrations, as already presented here for Rotterdam. In further work, the variability between the urban background concentrations and the concentrations at traffic/local scale should also be characterized, as it affects the estimation of population exposure.

RI-URBANS (www.RIURBANS.eu) is supported by the European Commission under the Horizon 2020 – Research and Innovation Framework Programme, H2020-GD-2020, Grant Agreement number: 101036245

This is a public document, available at the RI-URBANS website, https://riurbans.eu/work-package-4/#milestones-wp4, and distributed to all RI-URBANS partners for their use as well as submitted to European Commission as a RI-URBANS milestone M21 (M4.5).

2. Deterministic Models

To represent the heterogeneities of concentrations in cities, the urban concentrations estimated with the chemical transport model of WP3 at a 1 km x 1 km resolutions are downscaled to the street scale. Three approaches are used: a Gaussian approach with the model ADMS (Pilot cities Birmingham and Paris), an Eulerian approach with the street-network model MUNICH (Pilot city Paris) (Kim et al. 2022; Lugon et al. 2022) and a hybrid approach (Eulerian model, combined with a sub-grid Gaussian dispersion for street canyons) with the EPISODE-CityChem city-scale CTM model (Athens) (Karl et al., 2019; Lasne et al., 2023).

2.1 Paris Pilot

In PAR, regional-scale concentrations are simulated with the CHIMERE model (Menut et al. 2021) coupled to the street network MUNICH for NO_2, PM2.5, PM10, PNC-UFP, BC and other particle compounds (e.g. OA). The chain CHIMERE/MUNICH use the same aerosol module (SSH-aerosol, Sartelet et al. 2020) at both the regional and local scales, allowing to consider the dynamic of particles at all scales when computing the number concentrations. In the CHIMERE/MUNICH chain, the domain of simulation is discretized with a 1 km x 1 km resolution at the regional scale, with a zoom in the streets of Paris, which are explicitly represented using an eulerian approach avoiding double counting of traffic emissions when calculating the background and the street concentrations.

This modelling chain is compared to the chain used in Aiparif for operational purpose. It consists of CHIMERE for the regional scale and ADMS for the local-scale. Observation data of NO_2 are assimilated in the chain. Airparif employs the BLUE (Best Linear Unbiased Estimator) method for data assimilation. The Best Linear Unbiased Estimator enables the correction of air pollution mapping derived from the ADMS-Urban model. This technique involves merging the hourly outputs of the ADMS-Urban model with data from monitoring stations and relies on the model error covariance. Importantly, to support this approach, Airparif has developed a specific methodology for calculating realistic error covariances, which in turn facilitates the generation of uncertainty maps.

The CHIMERE/MUNICH chain use the Aiparif inventory of 2019 for activity sectors other than traffic and the CHIMERE/ADMS chain use the Airparif inventory of 2010. The traffic fleet is characteristic of summer 2022 in the CHIMERE/MUNICH chain and 2017 in the CHIMERE/ADMS chain.

The road traffic emissions data were produced based on the results obtained using the Heaven system originally developed in 2001 as part of the European project of the same name in partnership with the road traffic management departments of the City of Paris and the Direction Régionale de l'Equipement d'Ile-de-France. Since then, this system has been regularly updated on all its components: emission factors, vehicle fleets, traffic model, real-time countings, network, etc., in order to have the most recent information on vehicle emissions in the Paris region. The strength of this system is to use a traffic model that is corrected from the count data received in near real time. In the chain CHIMERE/MUNICH, the regional-scale traffic emissions were estimated by aggregating the local-scale emissions corrected from the local traffic counts.

Number emissions were estimated from the Airparif inventory using the methodology detailed in Sartelet et al. (2022).

RI-URBANS (www.RIURBANS.eu) is supported by the European Commission under the Horizon 2020 – Research and Innovation Framework Programme, H2020-GD-2020, Grant Agreement number: 101036245

2.1.1 Model evaluation compared to monitoring stations

The simulations are performed for June and July 2022. The comparisons are performed separately at background and traffic/street stations. Statistical evaluations are performed using Mean Bias, Mean Fractional Bias and Mean Fractional Error. In the Tables below "Airparif brut" refers to CHIMERE/ADMS simulations run by Airparif and "Airparif assim." refers to CHIMERE/ADMS simulations with data assimilation. Note that the assimilated data are also those to which the model to measurement comparison is performed, explaining the high model to measurement correlation observed for the Airparif assim. system. The NO_2 concentrations are well modelled at both background and traffic stations with simulated mean concentrations close to the measured value.

Table 1. *NO_2 model to measurement comparisons at background and traffic stations.*

NO_2	Stat. Type	Nb stat.	Simulation (µg m^{-3})	Obs. (µg m^{-3})	Mean Bias (µg m^{-3})	MFE (%)	MFB (%)	Correlation (%)
CHIMERE/MUNICH	Backgrd	19	16.6	15.5	1.1	34	7	55
Airparif brut	Backgrd	19	22.4		6.9	47	33	45
Airparif assim.	Backgrd	19	17.1		1.6	21	10	95
CHIMERE/MUNICH	Traffic	9	39.2	39.5	-0.1	26	5	62
Airparif brut	Traffic	9	38.3		-1.2	31	4	58
Airparif assim.	Traffic	9	36.0		-3.5	16	-8	94

For the model to measurement comparison of elemental carbon (EC) concentrations, the BC concentrations estimated from measurements were divided by 1.76 to estimate the EC concentrations, as suggested in Savadkoohi et al. (2023). As shown in Table 2, EC is well modelled at both the background and traffic sites using the CHIMERE/MUNICH chain. The $PM_{2.5}$ concentrations are overestimated compared to measurements in the CHIMERE/MUNICH chain (Table 3), probably because of uncertainties of the size distribution of non-exhaust emissions.

Table 2. *EC model to measurement comparisons at background and traffic stations.*

EC	Stat. Type	Nb stat.	Simulation (µg m^{-3})	Observation (µg m^{-3})	Mean Bias (µg m^{-3})	MFE (%)	MFB (%)	Correlation (%)
CHIMERE/MUNICH	Backgrd	3	0.5	0.5	0	36	12	55
CHIMERE/MUNICH	Traffic	3	1.3	1.2	0.1	40	20	48

RI-URBANS (www.RIURBANS.eu) is supported by the European Commission under the Horizon 2020 – Research and Innovation Framework Programme, H2020-GD-2020, Grant Agreement number: 101036245

Table 3. *$PM_{2.5}$ model to measurement comparisons at background and traffic stations.*

$PM_{2.5}$	Stat. Type	Nb stat.	Simulation (µg m^{-3})	Observation (µg m^{-3})	Mean Bias (µg m^{-3})	MFE (%)	MFB (%)	Correlation (%)
CHIMERE/MUNICH	Backgrd	4	8.6	8.1	0.5	30	13	69
CHIMERE/MUNICH	Traffic	3	12.1	11.1	1.0	25	11	72

Table 4. *$PNC_{>10}$ model to measurement comparisons at the urban background station "Les Halles" (central Paris) and at the suburban station "SIRTA".*

$PN_{>10}$ (# cm^{-3})	Stat. Type	Nb stat.	Simulation (µg m^{-3})	Observation (µg m^{-3})	Mean Bias (µg m^{-3})	MFE (%)	MFB (%)	Correlation (%)
CHIMERE/MUNICH	Urban Backgrd	1	7050	9186	-2136	38	-25	33
CHIMERE/MUNICH	Suburban	1	5794	5951	-157	26	-4	47

The number concentration PNC correspond to the concentration of number of particles of diameters about 10 nm. It is well modelled at the urban background site in central Paris and at the SIRTA suburban site (Table 4). Not only the number concentration is well modelled but the size distribution is well represented as well as shown in Figure 1, which represents dN/dlog d in the model and the measurements.

RI-URBANS (www.RIURBANS.eu) is supported by the European Commission under the Horizon 2020 – Research and Innovation Framework Programme, H2020-GD-2020, Grant Agreement number: 101036245

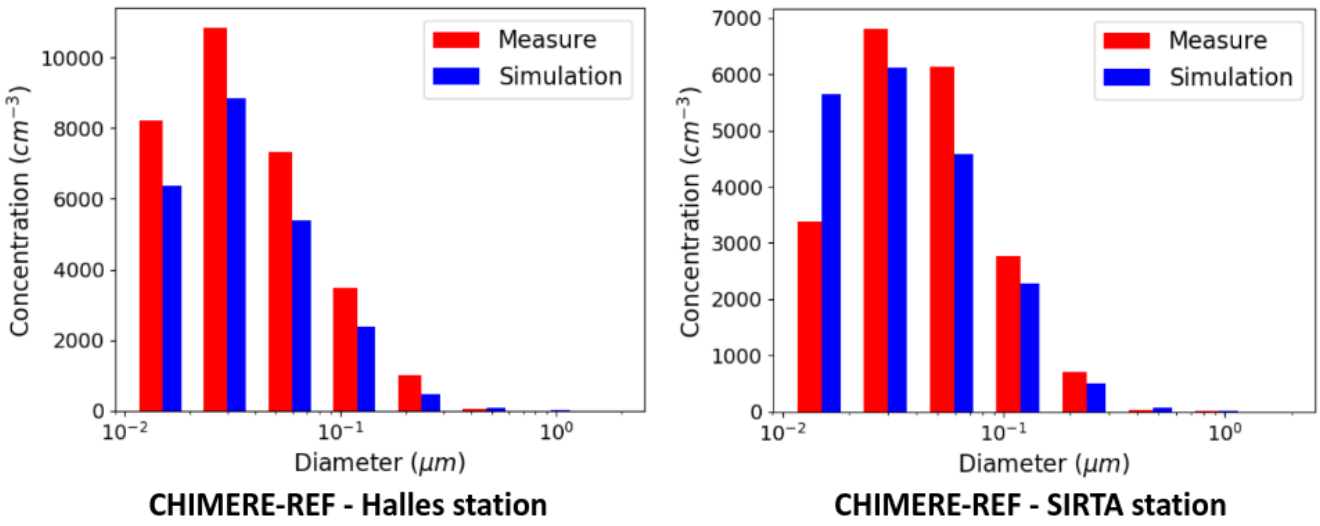

Figure 1. *Size distribution (PNSD) modelled and measured at the urban background station "Les Halles" in Central Paris (left panel) and at the SIRTA suburban station (right panel) (dN / dlog d).*

For PNC-UFP at traffic site, only a few weeks of measurements are available at Hôtel-de-Ville, in central Paris. The simulated $PN_{>10}$ compares well to the measurements, as shown in Figure 2.

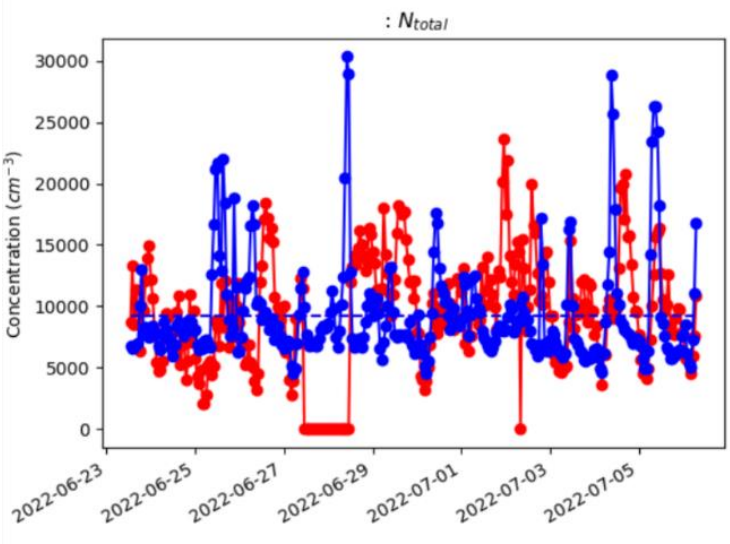

Figure 2. *Model to measurement comparisons of $PN_{>10}$ at the traffic site of Hôtel-de-Ville.*

2.1.2 Maps

Maps are plotted for the period July 2022, in Figure 3 for NO_2 concentrations, Figure 4 for EC concentrations and Figure 5 for $PN_{>10}$ concentrations. Concentrations of NO_2, EC and $PN_{>10}$ concentrations tend to be higher along roads and in streets with high traffic. For NO_2, as shown in Figure 3, the concentrations are lower in CHIMERE/MUNICH and Airparif assim. than in Airparif brut, which overestimates NO_2 concentrations (Table 1). This is because the emission inventory used in Airparif brut is older than in CHIMERE/MUNICH, and there is potential double counting of traffic emissions at the regional scale in the CHIMERE/ADMS chain. NO_2 concentrations simulated with CHIMERE/MUNICH are globally similar than Airparif assim., but they are higher in some streets. These higher

RI-URBANS (www.RIURBANS.eu) is supported by the European Commission under the Horizon 2020 – Research and Innovation Framework Programme, H2020-GD-2020, Grant Agreement number: 101036245

concentrations correspond well to measured concentrations, as shown by the lower mean bias in the model to measurement comparison of NO_2 concentrations at Bonapart station, which is in a street canyon in central Paris (Table 5).

	Airparif brut	Airparif assim.
CHIMERE/ADMS Airparif brut (left column) and Airparif assim. (right column)	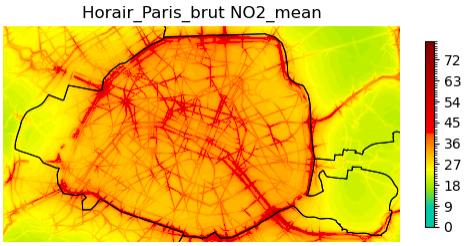	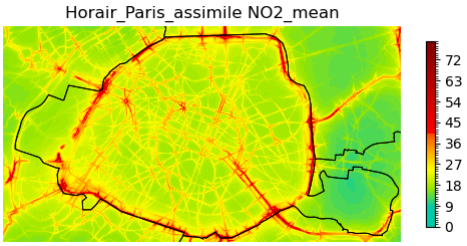
CHIMERE/MUNICH	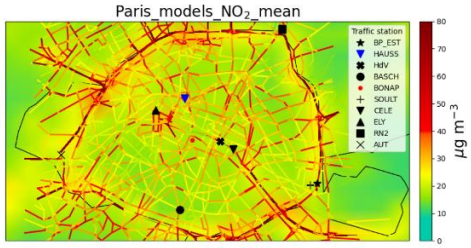	

Figure 3. *NO_2 concentrations simulated for July 2022 using the three different approaches: CHIMERE/ADMS (Airparif brut), CHIMERE/ADMS with assimilation of data at measurement sites (Airparif assim.), CHIMERE/MUNICH.*

Table 5. *NO_2 model to measurement comparisons at Bonapart station, a street canyon in central Paris.*

NO_2	Simulation (µg m^{-3})	Observation (µg m^{-3})	Mean Bias (µg m^{-3})	MFE (%)	MFB (%)	Correlation (%)
Airparif brut	36.1	29.9	6,2	29	22	62
Airparif assim.	26.5		-3,4	16	-1	92
CHIMERE/MUNICH	30.7		0,8	21	7	70

For EC, as shown in Figure 4, the concentrations are much higher in streets than in the rest of the domain, in agreement with the gradient observed between background and traffic stations, as shown in Table 2.

RI-URBANS (www.RIURBANS.eu) is supported by the European Commission under the Horizon 2020 – Research and Innovation Framework Programme, H2020-GD-2020, Grant Agreement number: 101036245

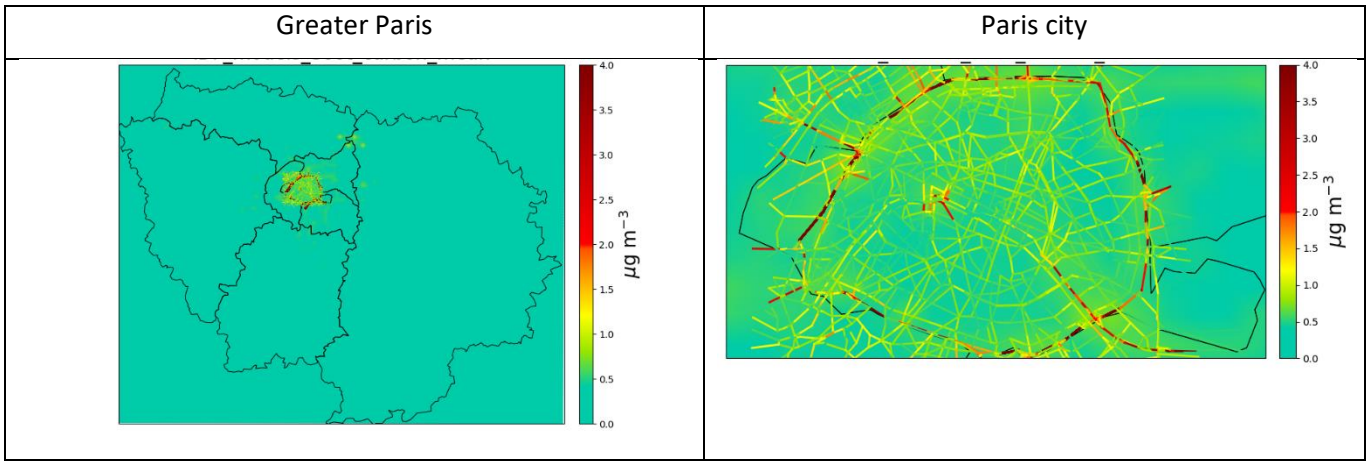

Figure 4. *EC concentrations simulated for July 2022 using CHIMERE/MUNICH*

$PNC_{>10}$ concentrations are less localised than EC concentrations, but they are much higher in areas of high traffic (Figure 5).

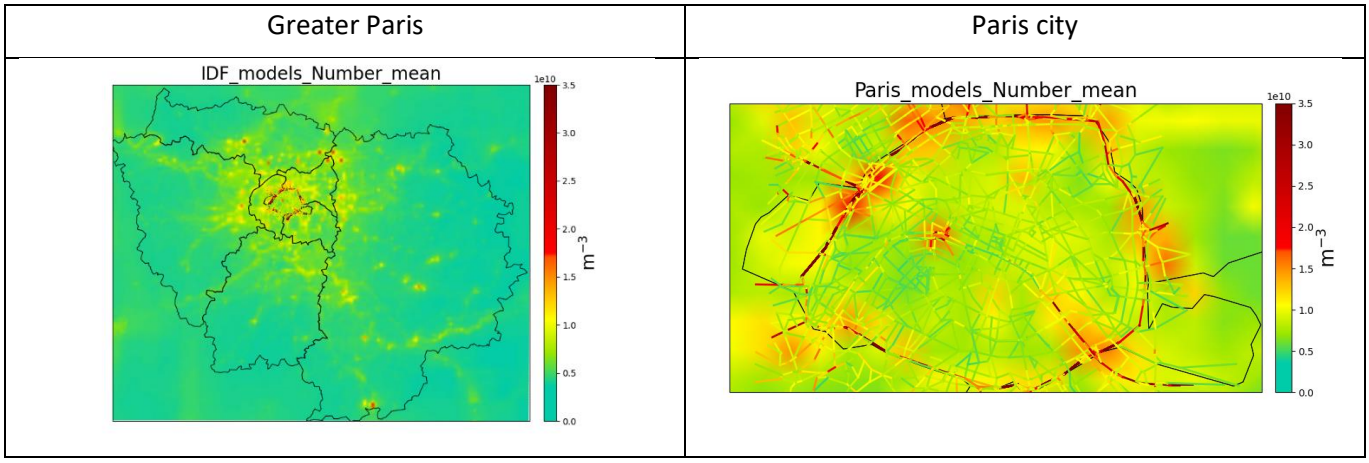

Figure 5. *$PN_{>10}$ concentrations simulated for July 2022 using CHIMERE/MUNICH.*

2.2 Birmingham Pilot

In Birmingham, a local scale ADMS-Urban model has been further developed based on the WM-Air modelling configuration for the year of 2016 for simulating the dispersion of NO_2 and $PM_{2.5}$ (Zhong et al., 2021). We have updated this ADMS-Urban model to the year of 2019 (the last normal year before Covid-19) and extended the modelling capability for the dispersion of nanoparticles and BC although further refinement is still needed. Here, we present the approach and results for nanoparticles as a case study.

2.2.1 Emission sources

Figure 6 shows emission sources included in the ADMS-Urban model, i.e. grid sources and explicit road sources. A grid emission inventory of nanoparticles has been developed by TNO, which was used in this modelling study. For road transport sources, we simulated major roads as explicit sources with non-resolved minor roads remaining in grid emissions of the transport sector to avoid double counting of road traffic emissions. Emissions were pre-

RI-URBANS (www.RIURBANS.eu) is supported by the European Commission under the Horizon 2020 – Research and Innovation Framework Programme, H2020-GD-2020, Grant Agreement number: 101036245

processed using EMIT (Atmospheric Emissions Inventory Toolkit) to produce formatted modelling inputs (CERC, 2021).

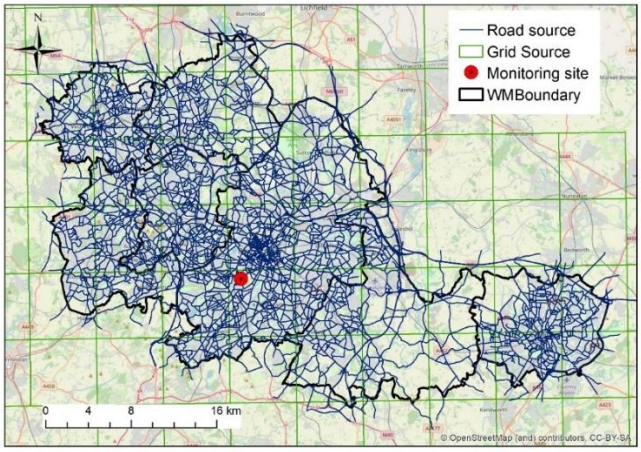

Figure 6. *Emission sources implemented in the ADMS-Urban model over the West Midlands (including Birmingham at the middle of the domain). Grid emission is at 6 km × 6 km resolution. The monitoring site at the Birmingham Air Quality Supersite (BAQS) to be used for model evaluation is also indicated.*

2.2.2 Model evaluation

The ADMS-Urban model was firstly run as a "Receptor" mode for the receptor location where the monitoring site was located (i.e. Birmingham Air Quality Supersite, BAQS). The Model Evaluation Toolkit (Stidworthy et al., 2018) was used to evaluate the model performance. Figure 7 shows a comparison of scatter plots for daily mean PNC_{10_100} (Particle Number Concentration between 10 and 100 nm). The model captured most of the features in daily means. Table 6 shows detailed model evaluation statistics compared with the measurement at the Birmingham Air Quality Supersite. Overall, the model generally performed well although with a slight underestimation.

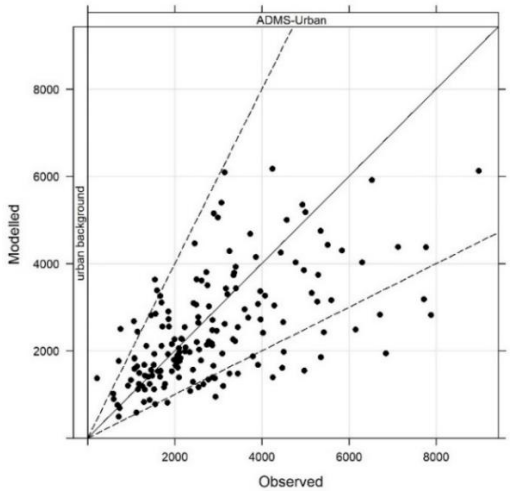

Figure 7. *Daily mean comparison between model and observation at BAQS for PNC-UFP between 10 and 100 nm (PNC_{10_100}, unit in # cm^{-3}) for the 2019 case.*

RI-URBANS (www.RIURBANS.eu) is supported by the European Commission under the Horizon 2020 – Research and Innovation Framework Programme, H2020-GD-2020, Grant Agreement number: 101036245

***Table 6**. Model evaluation statistics for the 2019 case compared with the measurement at the Birmingham Air Quality Supersite. Obs: measured PNC; Mod: modelled PNC; Fb: fraction bias; Fac2: fraction of modelling output within a factor of 2 of measurement; NMSE: normalised mean square error; R: correlation coefficient.*

Pollutant	Site Type	Obs (# cm^{-3})	Mod (# cm^{-3})	Fb	Fac2	NMSE	R
PNC_{10_100}	Urban background	2902	2487	-0.15	0.71	0.67	0.47

2.2.3 Maps

In order to generate maps, we need to run the ADMS-Urban model in the "Contour" mode. For a big computational domain, the splitting option using the task farming approach needs to be adopted and the domain was divided into 540 subdomains. The Linux version of the ADMS-Urban model was run on the supercomputer at the University of Birmingham using 540 cores each for a subdomain. Figure 8a shows annual concentration maps for PNC_{10_100} at 10 m × 10 m resolution for the 2019 case. PNC_{10_100} ranged from 2304 to 4478 # cm^{-3}. There were clear patterns of the influence of traffic emissions on the distributions of PNC with higher levels near major roads in the city centre and motorways. Lower levels of PNCs were observed in rural areas and regions far away from major roads. Figure 8b shows spatially aggregated annual maps for PNC_{10_100} at the electoral ward level. Ward level averaged PNC_{10_100} ranged from 2339 to 2894 # cm^{-3}. This spatial averaging would result in narrower ranges of PNCs, as both lowest and highest concentrations in the 10 m × 10 m map were not fully represented any more. However, the electoral ward level map is of importance and more relevant to health-related studies of air pollution as population and health data can be normally obtained at this level.

(a) (b)

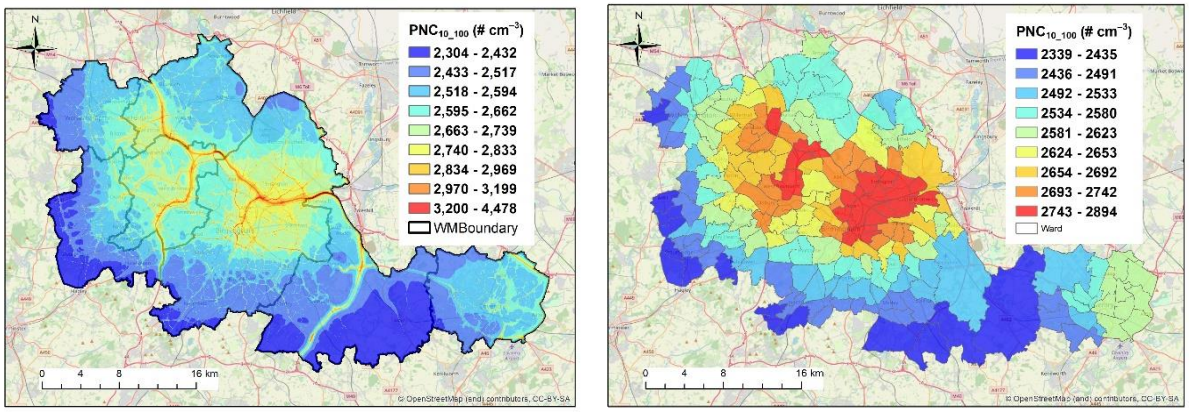

***Figure 8.** Annual PNC maps for PNC between 10 and 100 nm (PNC_{10_100}) (a) at 10 m × 10 m resolution and (b) at the electoral ward level for the 2019 case.*

2.3 Athens Pilot

In Athens, the variability of outdoor exposure to air pollution in the fine scale is assessed through applications of a numerical atmospheric model system already tested and applied in the frame of previous city-scale studies (Ramacher et al., 2021; Lasne et al., 2023). The core of the system is the chemistry transport model EPISODE-CityChem (Karl et al., 2019). Its comprehensive chemistry scheme is designed for treating complex atmospheric chemistry in urban areas and improved representation of the near-field dispersion. Input data (meteorology, boundary conditions, emissions) are heavily supported by Copernicus-related products. The model performs a specialized treatment on road and over the adjacent urban areas. Specifically, it is fed with hourly road network

RI-URBANS (www.RIURBANS.eu) is supported by the European Commission under the Horizon 2020 – Research and Innovation Framework Programme, H2020-GD-2020, Grant Agreement number: 101036245

emissions in a linear format, applies a Gaussian dispersion scheme in the street canyons, and an extra photochemical scheme over the greater area of road surfaces, gridded in 100 m-by-100 m cells. These two schemes are superimposed to the Eulerian treatment of atmospheric processes in the whole 3D urban domain, with a horizontal spatial resolution of 1 km and a 24-layered atmosphere up to 3.7 km.

$PM_{2.5}$ is accepted as the most harmful regulatory pollutant in terms of health effects (and especially excess mortality), while NO_2 is a good tracer for traffic-induced pollution. Given that the focus of this pilot is on urban health, the model outputs used for this study are for $PM_{2.5}$ and NO_2.

2.3.1 Model evaluation compared to monitoring stations

Comparison of predictions against available hourly data for NO_2 (regulatory network) and $PM_{2.5}$ (enriched with data from low-cost sensors from the Panacea RI) are performed. The year 2019 is selected as a recent year, free of Covid-related activity restrictions, and with a wind field representative of 2016-2020. Evaluation statistics, comparative time-series plots and selected outputs from the application of the benchmarking methodology developed in the framework of the Forum for Air Quality Modelling in Europe (FAIRMODE) are provided below.

Table 7. *Final model performance metrics for NO_2 predicted concentration levels in Athens (Greece), when compared with measurements from the National regulatory network. The statistics are derived from mean daily values for the entire year 2019.*

Station	**Observed** ($\mu g\ m^{-3}$)	**Modeled** ($\mu g\ m^{-3}$)	**Mean Bias** (MB, $\mu g\ m^{-3}$)	**Root Mean Square Error** (RMSE, $\mu g\ m^{-3}$)	**Correlation Coefficient** (r)	**No of pairs**
AGP	12.8	10.6	-2.2	7.6	0.49	365
KOR	14.9	11.2	-3.7	6.5	0.75	365
LIO	21.1	22.6	1.5	10.7	0.75	309
LYK	19.9	14.6	-5.3	11.3	0.74	296
MAR	25.6	9.3	-16.3	19.4	0.65	363
PER	28.1	15.4	-12.7	16.6	0.73	365
SMY	27.0	15.6	-11.4	16.1	0.62	228
THI	28.7	16.7	-12.0	15.5	0.63	272
THR	6.8	5.2	-1.6	5.1	0.70	226
Mean (Background stations)	**20.5**	**13.5**	**-7.1**	**12.1**	**0.67**	**2789 (sum)**
ARI	42.7	59.2	16.5	24.7	0.48	365
ATH	46.5	47.0	0.5	16.3	0.40	268
PAT	73.5	42.2	-31.3	34.5	0.68	359
PIR	62.9	22.5	-40.5	42.5	0.55	242
Mean (Traffic stations)	**56.4**	**42.7**	**-13.7**	**29.5**	**0.53**	**1234 (sum)**
ELE	25.2	33.8	8.7	14.3	0.69	355
GEO	34.2	21.0	-13.2	17.9	0.59	323
Mean (Industrial stations)	**29.7**	**27.4**	**-2.3**	**16.1**	**0.64**	**678 (sum)**
Mean (all stations)	**31.3**	**23.1**	**-8.2**	**17.3**	**0.63**	**4701 (sum)**

RI-URBANS (www.RIURBANS.eu) is supported by the European Commission under the Horizon 2020 – Research and Innovation Framework Programme, H2020-GD-2020, Grant Agreement number: 101036245

***Table 8**. as Table 7, but for $PM_{2.5}$ (enriched with low-cost sensor measurements).*

Station	**Observed** (μg m^{-3})	**Modeled** (μg m^{-3})	**Mean Bias** (MB, μg m^{-3})	**Root Mean Square Error** (RMSE, μg m^{-3})	**Correlation Coefficient** (r)	**No of pairs**
AGP	11.9	12.5	0.6	4.5	0.62	325
GYZ	13.1	14.8	1.7	5.2	71	228
HAI	12.8	12.2	-0.6	5.1	0.67	158
HAL	14.0	12.9	-1.2	8.0	0.54	215
KER	12.6	12.7	0.1	5.1	0.65	228
LYK	16.4	13.4	-3.0	7.6	0.54	285
MEL	11.4	12.2	0.8	4.4	0.59	224
PEF	12.4	13.7	1.3	5.3	0.61	228
THR	13.2	11.3	-1.3	5.3	0.51	274
VOU	10.1	11.5	1.4	4.0	0.62	178
ZEA	14.4	13.0	-1.4	6.5	0.56	228
Mean (Background stations)	**12.9**	**12.7**	**-0.2**	**5.6**	**0.60**	**2571 (sum)**
ARI	19.3	20.3	1.0	6.9	0.67	335
PIR	17.6	13.7	-3.9	8.8	0.51	299
Mean (Traffic stations)	**18.5**	**17.0**	**-1.5**	**7.8**	**0.59**	**634 (sum)**
ELE (Industrial)	18.5	16.2	-2.3	6.3	0.63	281
Mean (all stations)	**14.1**	**13.6**	**-0.5**	**5.9**	**0.60**	**3486 (sum)**

(a)

RI-URBANS (www.RIURBANS.eu) is supported by the European Commission under the Horizon 2020 – Research and Innovation Framework Programme, H2020-GD-2020, Grant Agreement number: 101036245

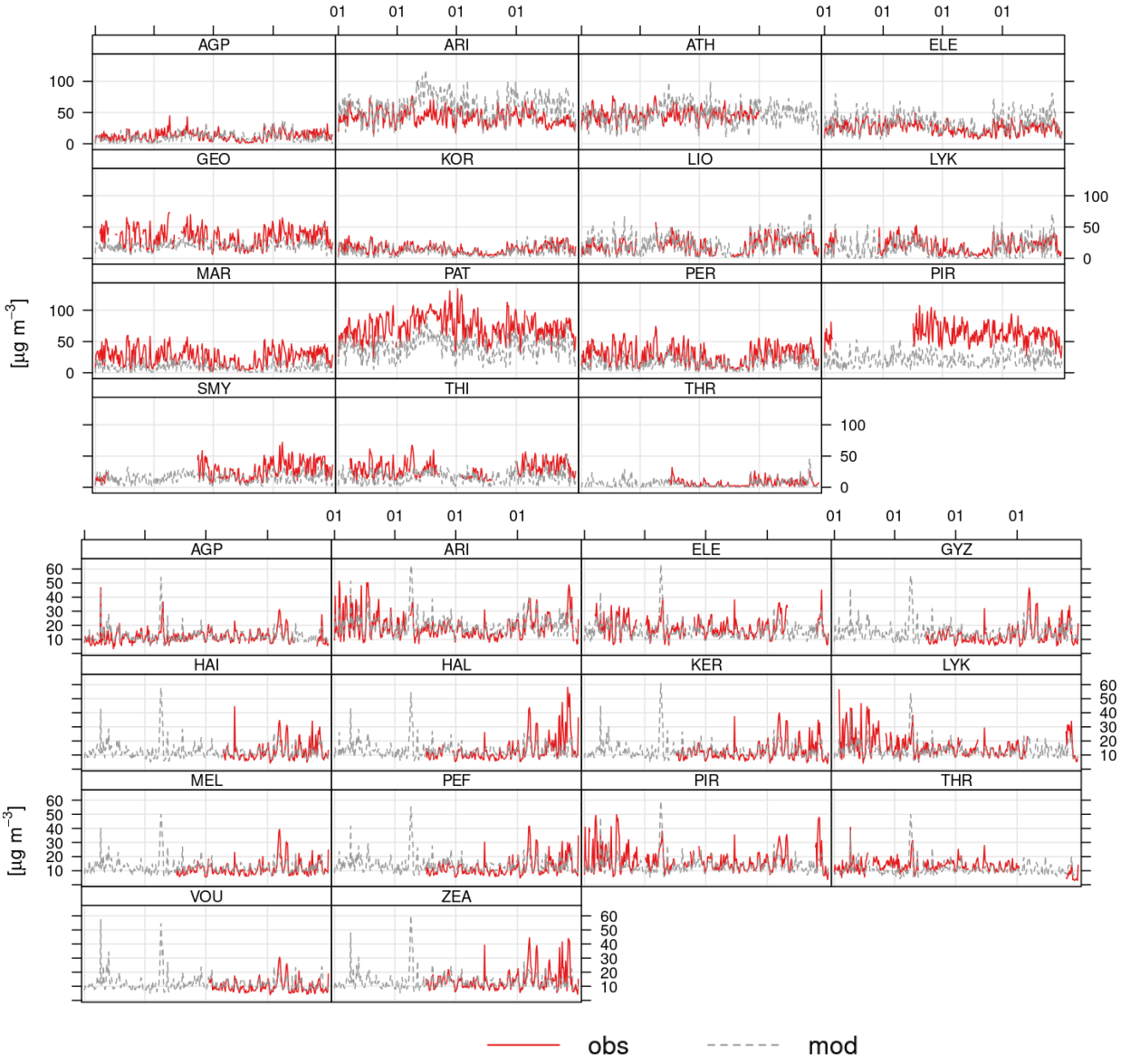

(b)

Figure 9. *Daily timeseries of observed and modelled values for all monitoring stations, for 2019, for (a) NO_2, (b) $PM_{2.5}$.*

RI-URBANS (www.RIURBANS.eu) is supported by the European Commission under the Horizon 2020 – Research and Innovation Framework Programme, H2020-GD-2020, Grant Agreement number: 101036245

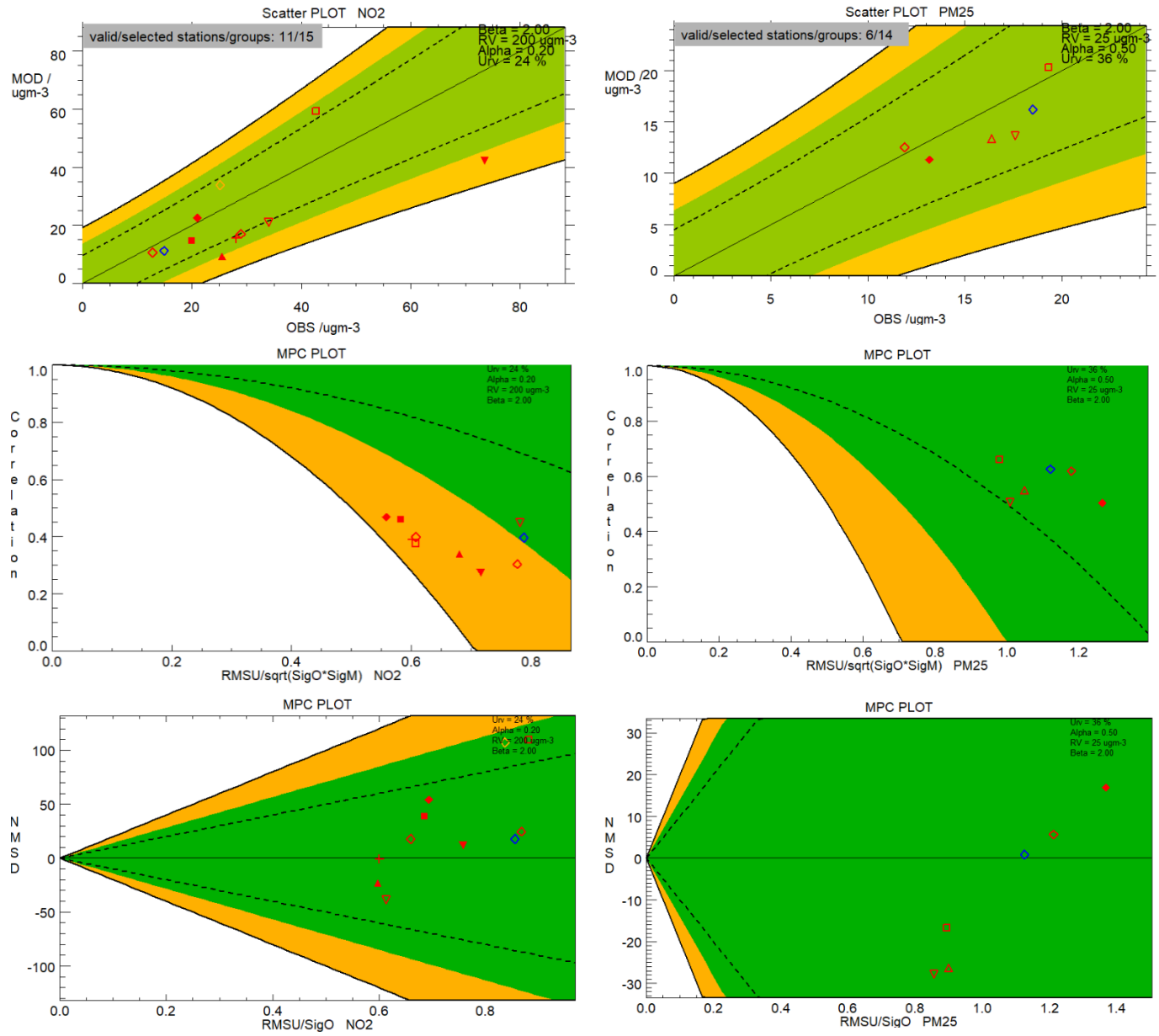

Figure 10. *Model performance criteria for Athens city-scale simulations (2019), associated with: model vs observation (scatter plot) of mean annual values (top row), correlation coefficient (correlation vs RMSU/v(SigO*SigM), middle row) and standard deviation (normalised mean standard deviation vs RMSU/SigO, bottom row), for (a) hourly values of NO_2, (b) mean daily values of $PM_{2.5}$. The evaluation has used the benchmarking methodology developed in the framework of the Forum for Air Quality Modelling in Europe (FAIRMODE).*

RI-URBANS (www.RIURBANS.eu) is supported by the European Commission under the Horizon 2020 – Research and Innovation Framework Programme, H2020-GD-2020, Grant Agreement number: 101036245

2.3.2 Maps

AQ mapping of the whole simulation domain as annual averages of NO_2 and $PM_{2.5}$ is presented in Figure 11. Additional mapping of air pollution concentrations, spatially targeting the near-road areas (at the spatial scale of 100m) and temporally focusing on representative hours of pollution peaks during the summer and winter period is given in Figure 12 (for NO_2) and Figure 13 (for $PM_{2.5}$).

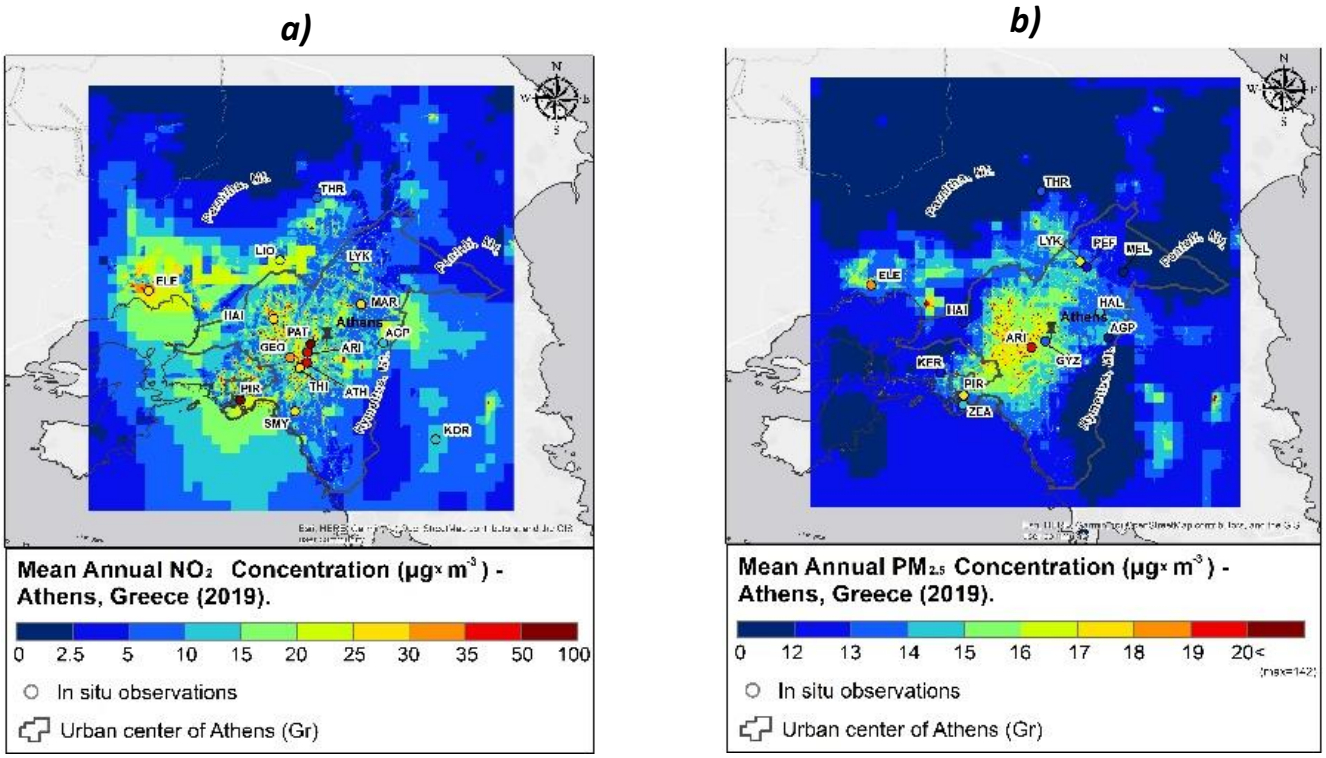

Figure 11. *The spatial distribution of NO_2 (a) and $PM_{2.5}$ (b) mean annual predicted values over Athens (Greece) during 2019. The color-coded points represent measured concentrations.*

RI-URBANS (www.RIURBANS.eu) is supported by the European Commission under the Horizon 2020 – Research and Innovation Framework Programme, H2020-GD-2020, Grant Agreement number: 101036245

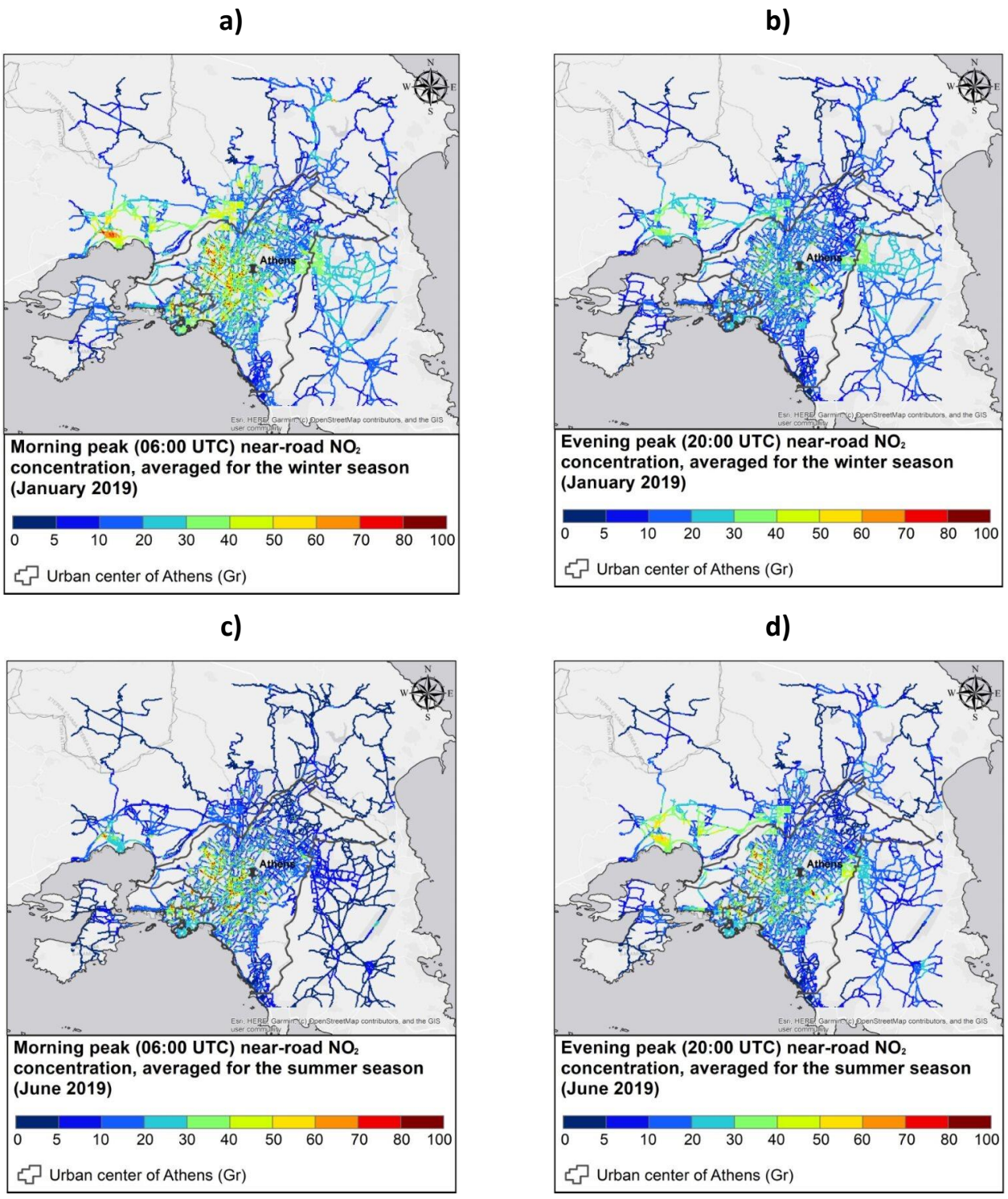

***Figure 12**. Hourly mapping of NO_2 concentrations (μg m^{-3}) along traffic axes and streets, averaged for the winter (January 2019, a and b) and summer (June 2019, c and d).*

RI-URBANS (www.RIURBANS.eu) is supported by the European Commission under the Horizon 2020 – Research and Innovation Framework Programme, H2020-GD-2020, Grant Agreement number: 101036245

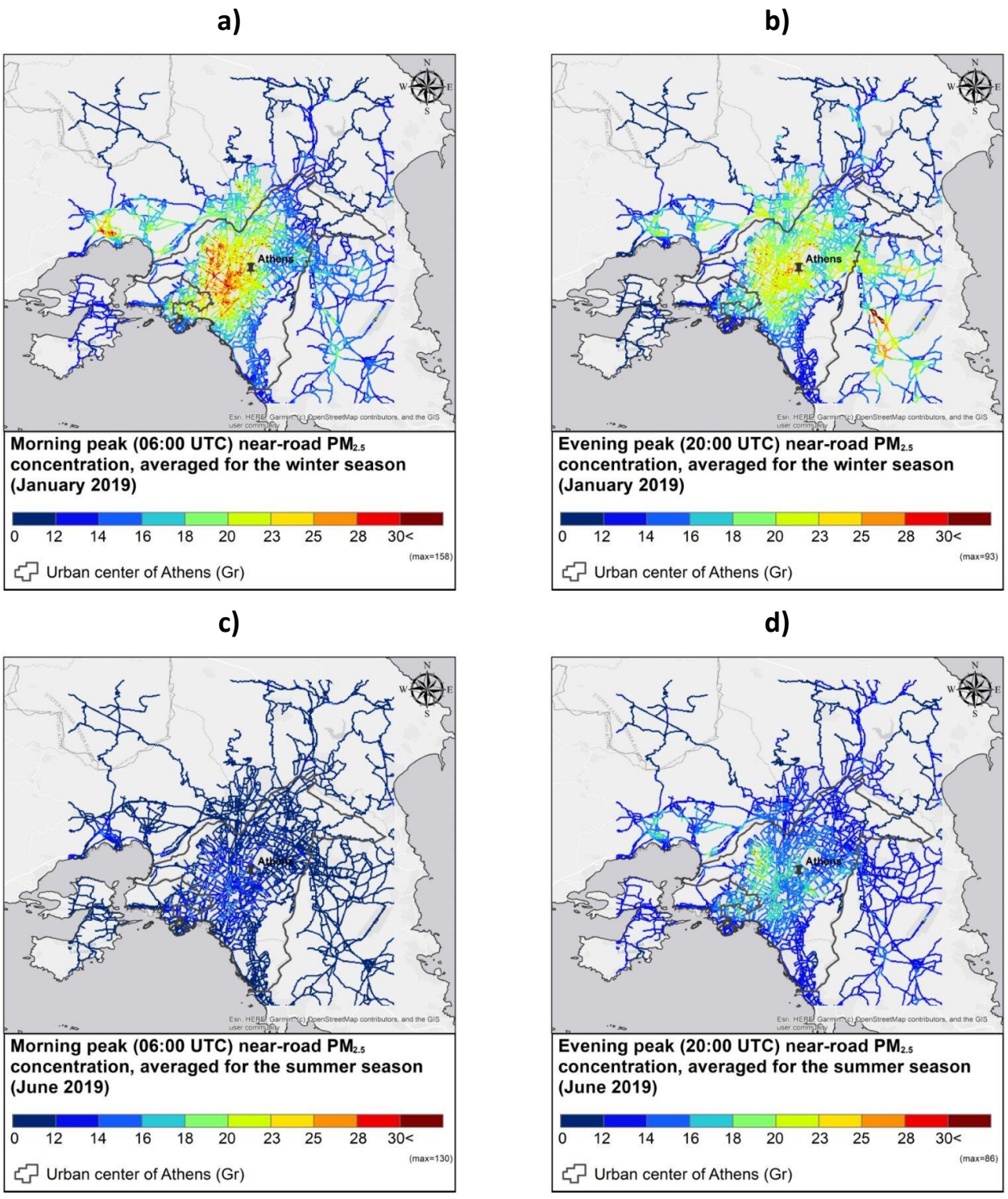

***Figure 13**. Hourly mapping of $PM_{2.5}$ concentrations (μg m^{-3}) along traffic axes and streets, averaged for the winter (January 2019, a and b) and summer (June 2019, c and d).*

Vertical concentration profiles can be provided upon demand for selected points of the urban area of Athens and representative hours.

RI-URBANS (www.RIURBANS.eu) is supported by the European Commission under the Horizon 2020 – Research and Innovation Framework Programme, H2020-GD-2020, Grant Agreement number: 101036245

3. Analysis of mobile monitoring and/or citizen observations

Mobile monitoring and/or citizen observations can be used with land-use regression models or machine learning to produce maps.

3.1 Rotterdam Pilot

In ROT, mobile monitoring is performed using a car and combined w*ith measurements by cyclists or* pedestrians with portable instruments for nanoparticles and BC. A key input is vertical gradients using remote sensing, building on regional background measurements. During the two campaigns with mobile measurements, large spatial gradients were observed.

3.1.1 Car measurements

We used a car to measure the ambient concentrations of NO_2, BC and $PNC_{<10}$-UFP during two seasons; one in November-December 2022 and in May-July 2023. The car was equipped with lab-grade 1 Hz NO_2 (CAPS, Aerodyne Research Inc., USA), 1 Hz BC (AE33, Magee Scientific), and 1 Hz PNC-UFP (EPC 3783, TSI) monitors measuring simultaneously. A Global Positioning System (GPS) (G-Star IV, GlobalSat, Taiwan) was used to record the location of the car, which was linked to the measuring equipment via date and time. The measurements were mainly carried out between 08.00 to 22.00 hours every day in the study period (including some weekend days) in different parts of the city. The aim was to reduce possible space and time autocorrelation. Therefore, there is no need to temporally correct the measurements.

The data was winsorised to the 2.5^{th} and the 97.5^{th} percentile. That is, measured concentration levels below the 2.5th percentile and above the 97.5th percentile were “replaced” by the respective percentile values (Kerckhoffs et al. 2022). This procedure is done to balance the unduly influence of extreme values, while allowing very high pollution values. For averaging, the data was first assigned to the nearest street and aggregated over each 50-meter (min: 30m and max: 60m) street segment per individual drive day. In total ~40000 street segments were measured.

3.1.2 Comparison with reference stations

Car measurements were extensively compared with reference monitors from the Dutch Government (serviced by GGD) before the start of the Rotterdam campaign in Amsterdam. This was done by parking the car as close the measurement station as possible and measure air pollution for at least one hour. Results show excellent correlation between reference measurements and car measurement for all pollutants, see Figure 14. Correlation statistics are based on 60 min average concentrations and were performed on 12 different days.

RI-URBANS (www.RIURBANS.eu) is supported by the European Commission under the Horizon 2020 – Research and Innovation Framework Programme, H2020-GD-2020, Grant Agreement number: 101036245

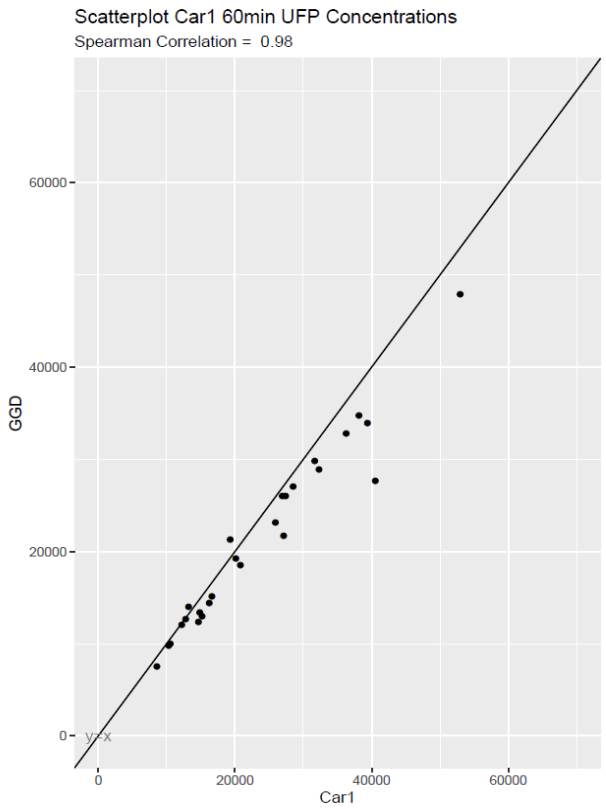

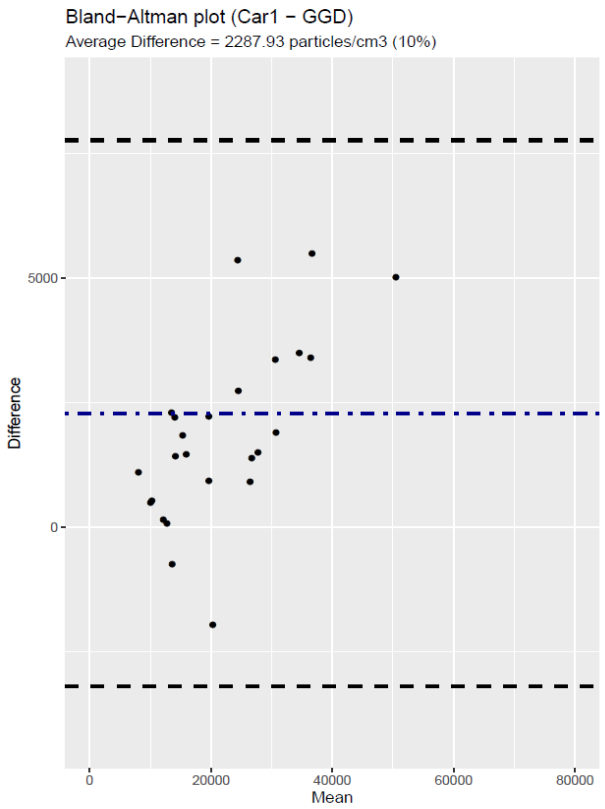

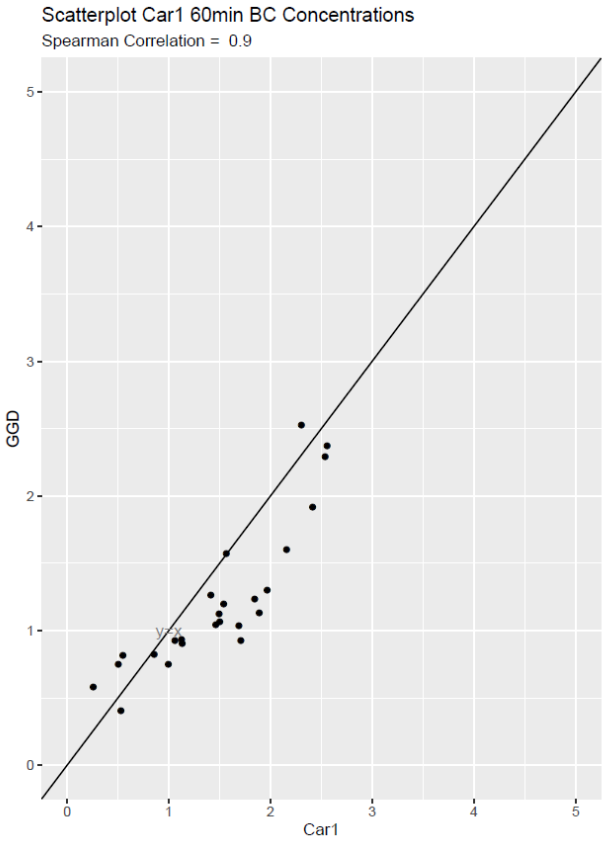

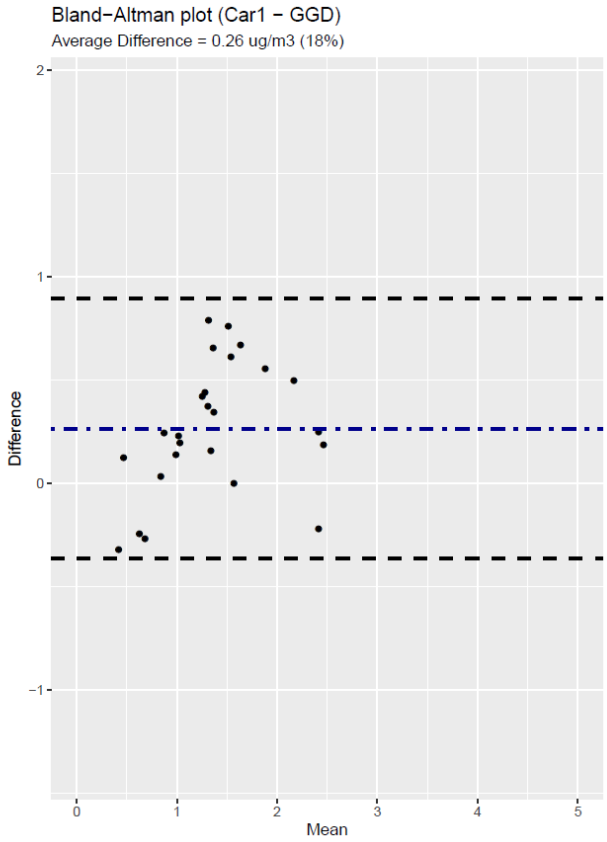

RI-URBANS (www.RIURBANS.eu) is supported by the European Commission under the Horizon 2020 – Research and Innovation Framework Programme, H2020-GD-2020, Grant Agreement number: 101036245

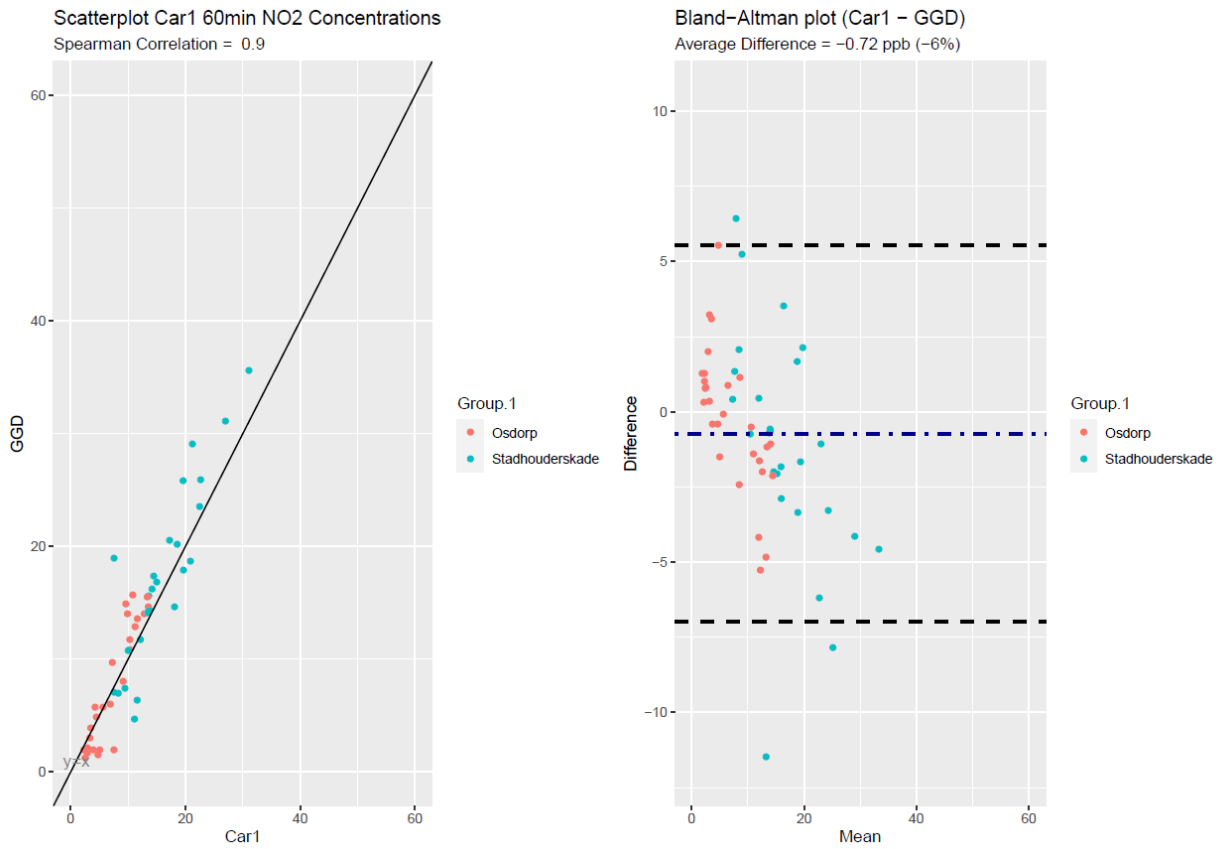

***Figure 14**. Comparisons to reference monitors prior to the measurement campaign.*

3.1.3 Models and maps based on car measurements

For the maps, we used linear mixed-effect models. These models use fixed effects estimated based on determinants from a linear regression model (SLR) and random intercepts for all individual street segments (random-effect model). Such model combines the advantages of "data-only" mapping and LUR modelling, meaning that all individual measurements can influence the output of the fixed-effect model based on the measured between and within-street segment concentration variation. The mixed-effect modelling framework has been extensively explained and validated, demonstrating the feasibility of the adopted approach to develop high-resolution NO_2 concentration maps for Amsterdam and Copenhagen with better performance than data-only and LUR-only approaches.

Spatial patterns are highlighted in Figures 15, 16 and 17. As expected, the major roads in and around Rotterdam have the highest concentrations of air pollution. For PNC-UFP, this is more pronounced on the highways than for the other two pollutants. UFPs quickly transform through physicochemical processes, like coagulation or condensation and can reach background levels within 300 meters of a highway, with even sharper gradients for the smaller particles. For NO_2 and BC, elevated concentrations are mainly found towards the city centre.

We also show ratios between pollutants in Figures 18, 19 and 20. They are based on a quantile division of predictions of two pollutants and their relative loading. Thus, each of the four colours in the 2x2 box represent an equal number of road segments. For all pollutants, as expected, the major roads have the highest concentrations of air pollution. For PNC-UFP, this is more pronounced on the highways than the other two pollutants. PNC-UFPs quickly transform through physicochemical processes, like coagulation or condensation and can reach background levels within 300 m of a highway, with even sharper gradients for the smaller particles. Since the traffic volume on

RI-URBANS (www.RIURBANS.eu) is supported by the European Commission under the Horizon 2020 – Research and Innovation Framework Programme, H2020-GD-2020, Grant Agreement number: 101036245

highways is much more than on other roads, there are many fresh particles, resulting in the fact that only highways show up as the main hotspot for PNCUFP, whereas this is more variable for NO_2 and BC.

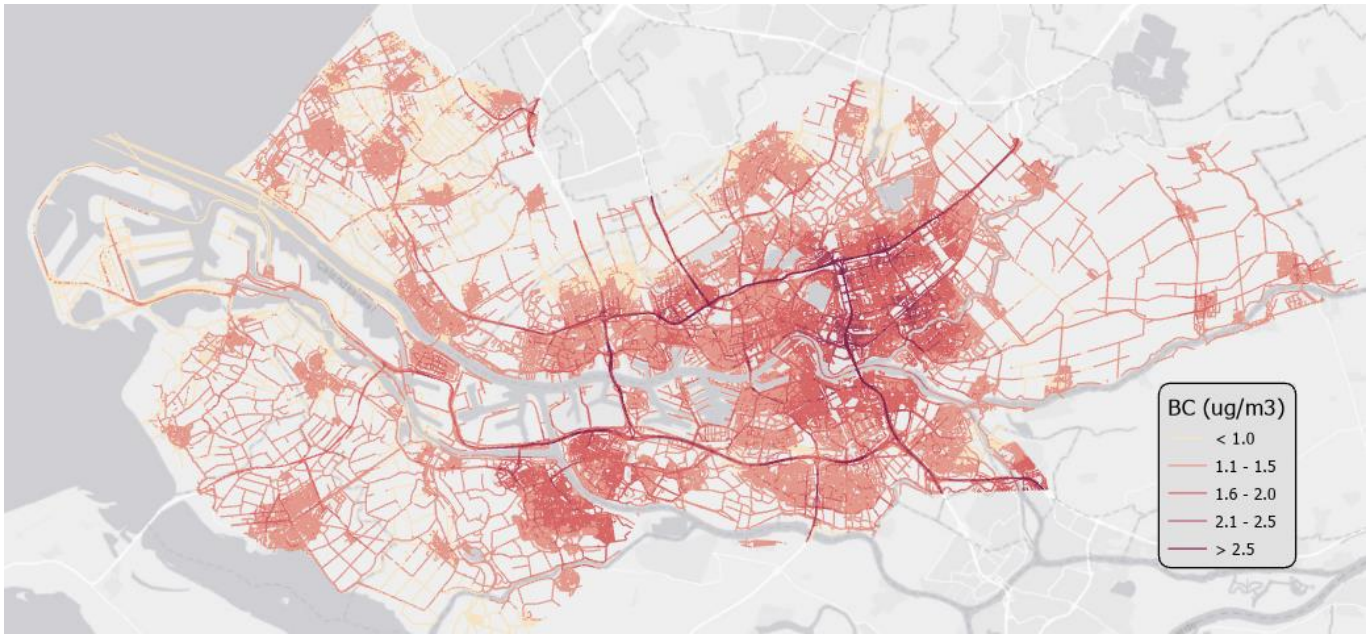

Figure 15. *Mixed-effect model predictions for BC concentration levels in Rotterdam.*

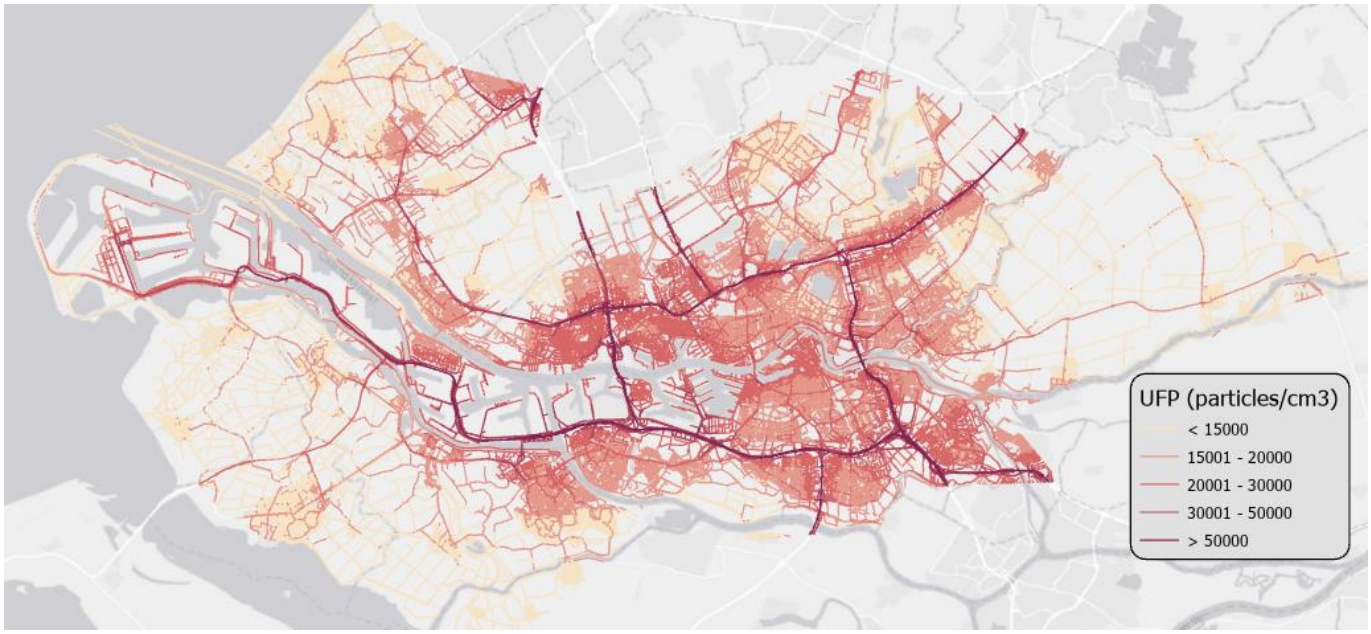

Figure 16*. Mixed-effect model predictions for PNC-UFP concentration levels in Rotterdam.*

RI-URBANS (www.RIURBANS.eu) is supported by the European Commission under the Horizon 2020 – Research and Innovation Framework Programme, H2020-GD-2020, Grant Agreement number: 101036245

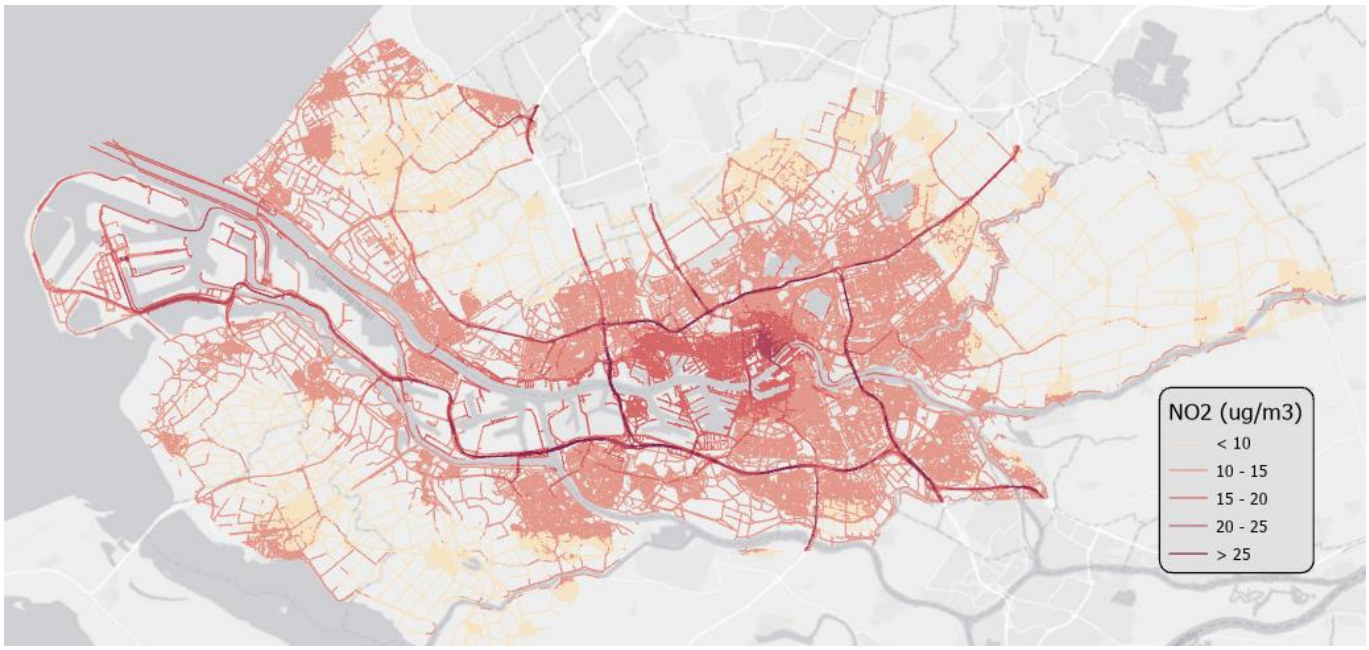

Figure 17. *Mixed-effect model predictions for NO_2 concentration levels in Rotterdam.*

Figure 18. *Ratio between predicted NO_2 concentrations and PNC-UFP concentrations in Rotterdam. Each of the four colours in the 2x2 box represent an equal number of road segments.*

RI-URBANS (www.RIURBANS.eu) is supported by the European Commission under the Horizon 2020 – Research and Innovation Framework Programme, H2020-GD-2020, Grant Agreement number: 101036245

Figure 19. *Ratio between predicted NO_2 concentrations and BC concentrations in Rotterdam. Each of the four colours in the 2x2 box represent an equal number of road segments.*

Figure 20*. Ratio between predicted PNC-UFP concentrations and BC concentrations in Rotterdam. Each of the four colours in the 2x2 box represent an equal number of road segments.*

3.1.4 Mobile measurements with citizens

Within RI-URBANS mobile mapping with citizens is also used to collect data on a high spatial resolution. The approaches rely on mobile measurements with citizens to derive spatial air pollution maps. Mobile measurements can contribute to understand spatial variability of short-living constituents of air pollution from a diversity of pollution sources.

The monitoring campaign in Rotterdam is performed with volunteers, who are all employees of DCMR or the city of Rotterdam. They are asked to measure during their daily bicycle commutes. Before the measurement campaign, a training session was organized for the volunteers. Measurements were performed in winter (November 2022 – February 2023) and repeated in spring/summer 2023 (June – July 2023).

Measurements are based on the airQmap approach; more information on the approach and previous studies can be found on https://www.airQmap.com. Measurements of BC are performed using a microaethalometer (microAeth®, AE51, AethLabs) and a GPS. BC is measured at 1s temporal resolution and a flow rate of 150 mL min-

RI-URBANS (www.RIURBANS.eu) is supported by the European Commission under the Horizon 2020 – Research and Innovation Framework Programme, H2020-GD-2020, Grant Agreement number: 101036245

1. To reduce the noise in BC measurements, the ONA (Optimized Noise-reduction Averaging, Hagler et al., 2011) algorithm was used with an attenuation threshold of 0.05. The geo-tagged measurements were aggregated (trimmed mean) and attributed to fixed points 20 m apart from each other along the cycling route.

The data are currently processed in aggregated (measured) maps and can be used to compare with modelled results or as input for LUR models.

3.2 Bucharest Pilot

In BUC, mobile monitoring was performed using a car with portable instruments for PNC-UFP, different particle matter fractions (PM_1, $PM_{2.5}$, PM_{10}) and gaseous compounds (NO_2, SO_2). Two campaigns with mobile measurements have been conducted on warm and cold seasons on representative traffic roads inside the city, touching residential, industrial and commercial areas, as well as sub-urban areas.

3.2.1 Tests and instruments inter-comparison

Several tests and mobile sensors inter-calibrations against the reference instrumentation at RADO-Bucharest site have been conducted prior to the car measurements campaign. The test includes monthly comparison against a reference instrument at site. For both particles and gaseous concentrations, the correlations are above 0.75.

The relative humidity influence on the aerosol measurements has been considered and during tests it had been raised the necessity to use a drying system before the UFP sensor to keep the relative humidity lower than 40% during the warm season measurements.

3.2.2 Car measurements

The car measurements campaigns took place during two seasons: 04 May –13 July (warm period) and 18 January - 28 February (cold period). The car has been equipped with different sensors measuring simultaneously: a UFP sensor (Naneos Partector 2, 1 s), particle and gaseous sensors (Ecomesure EcomTrek - 10 s and/or Sniffer4D V2, 1 s) and a GPS (Navilock NL-442U, 1s) to independently save the geographic coordinates.

Car route had been designed to pass main traffic roads, residential areas as well as industrial and commercial areas representative for Bucharest city, with a total length of 100 Km. The measurements durations were approximatively 8 hours starting from 8:30 AM local time in order to catch rush hours, but also less intense traffic during the mid-day of working days. At least full 15 measurements routes were performed during each campaign, in different temperature conditions.

The data has been filtered to remove the spikes and only keep the consistent measurements. The filtering used a moving average window on 3 datapoints, the concentrations higher and lower more than 1.5 times than the mean being removed.

3.2.3. Models and maps based on car measurements

The ESCAPE Land Use Regression models (Schmitz et al., 2019) together with PyLUR tool and QGIS (Ma et al, 2020) it was set up in order to retrieve the pollutants maps and tested on BUC warm period campaign data. The goal is to retrieve the air pollution maps for Bucharest area in order to assess the contribution of diverse area to air pollution, the gradients on particle concentrations between areas and related exposure along roads in different seasons or atmospheric conditions. The mixed effect model has been also tested, using the mean value from the fixed effect model (LUR) together with the pollutant variability (intercept of mean standard deviation values) for all individual street segments at 1 minute.

RI-URBANS (www.RIURBANS.eu) is supported by the European Commission under the Horizon 2020 – Research and Innovation Framework Programme, H2020-GD-2020, Grant Agreement number: 101036245

The average concentration of ultrafine particles on the mobile route during the warm and cold periods present a large spatial gradient, which highlights the personal exposure to ultrafine particles along the roads. Both, UFP and NO_2 concentrations presented significant gradients over short distances, with differences up to a factor of 2 in the mean.

Maps representing the spatial variability of NO_2, UFP and PM_{10} during warm period are presented in Figures 21, 22 and 23. The main traffic roads represent the hot spots for the NO_2 maps, while the anthropogenic agglomerations for the particle maps. Highest NO_2 concentrations are observed, as expected, on the Bucharest ring road and principal city traffic routes, with noticeable increase of concentrations in the city centre, where the intensity of the traffic persists for the entire day. Pronounced concentrations are depicted in the case of UFP and PM_{10} on some important traffic routes as well, but mainly on the industrial area and anthropogenic agglomerations. The spatial variation of particles in the city area is significant, with important number of small particles and high mass concentration of bigger particles on the high populated residential areas.

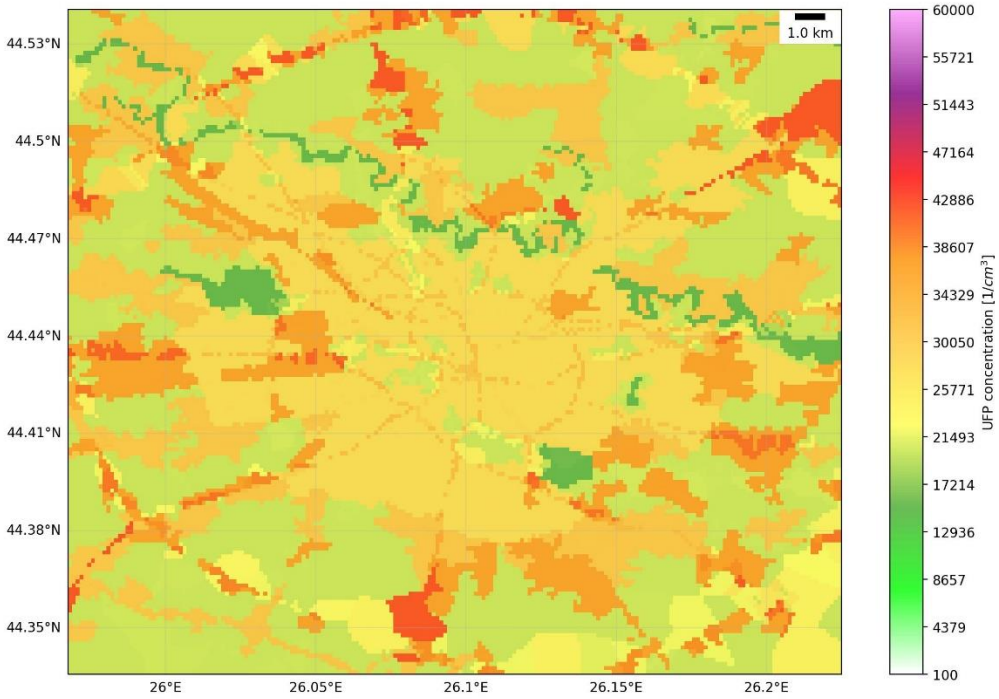

***Figure 21**. Model predictions for PNC-UFP concentration levels in Bucharest during warm period.*

RI-URBANS (www.RIURBANS.eu) is supported by the European Commission under the Horizon 2020 – Research and Innovation Framework Programme, H2020-GD-2020, Grant Agreement number: 101036245

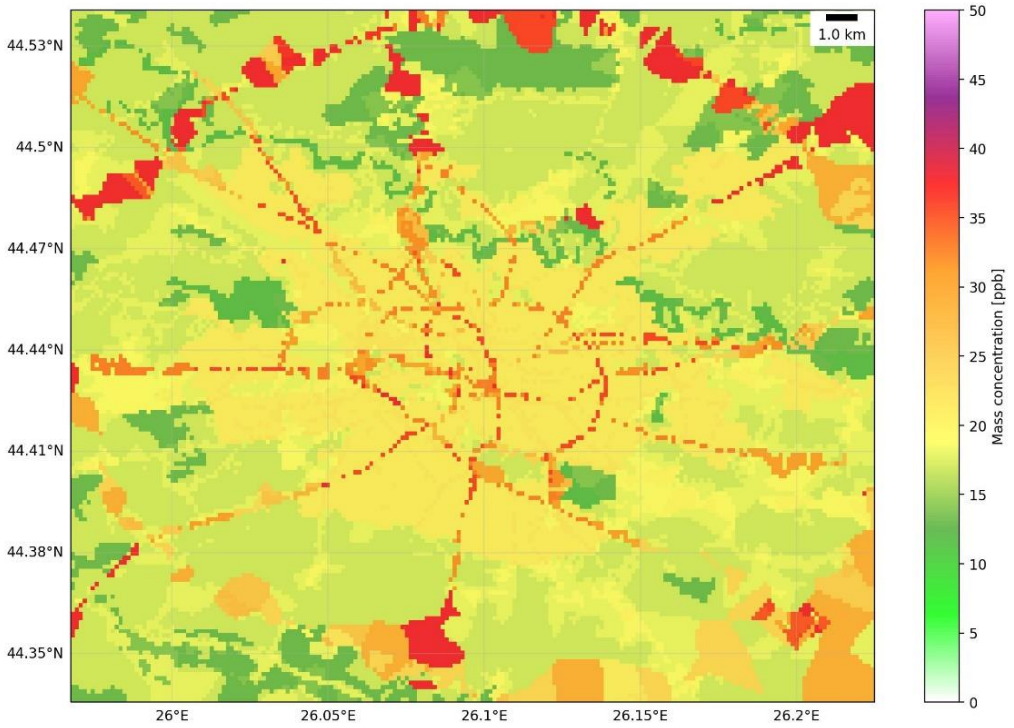

Figure 22. *Model predictions for NO_2 concentration levels in Bucharest during warm period.*

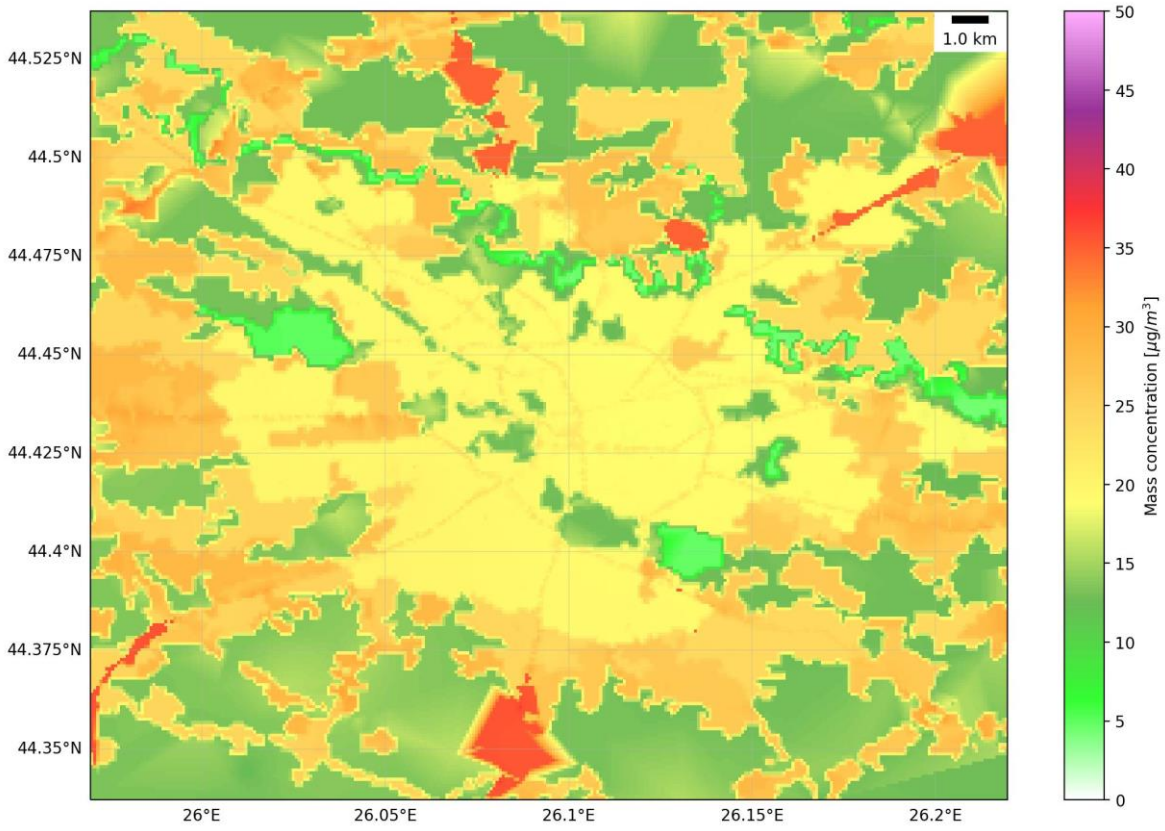

Figure 23. *Model predictions for PM_{10} concentration levels in Bucharest during warm period.*

The model performance has been evaluated for UFP measurements versus predicted values at one-hour average (Figure 24). Overall, the model captures well the variability of the particle during the warm period. In the case of

RI-URBANS (www.RIURBANS.eu) is supported by the European Commission under the Horizon 2020 – Research and Innovation Framework Programme, H2020-GD-2020, Grant Agreement number: 101036245

lower concentrations, the model sub-estimated the mean measurements values, while the highest values are rather supra-estimated.

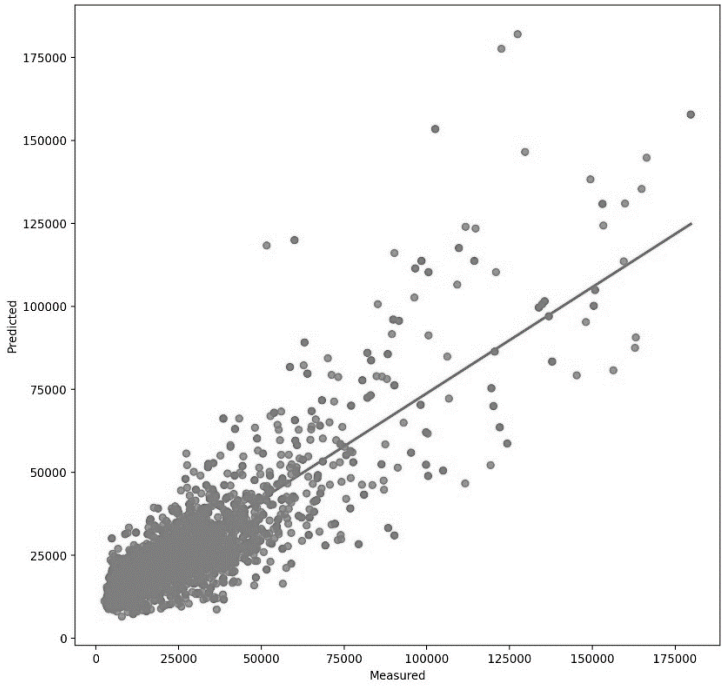

Figure 24. *Model evaluation using the hourly mean concentrations of PNC-UFP on model and measurements in Bucharest warm period.*

Also, the model performance has been evaluated for NO_2 and PM_{10} using the hourly data available at the Romanian National Air Quality Monitoring Network (8 stations representative for urban, industrial and suburban) and at RADO-Bucharest ACTRIS site (PM10). Mean values of root mean square error (RMSE) and correlation coefficient are evaluated using the data from May to August 2022. Overall, the model performed well, NO_2 values are slightly overestimated and PM_{10} underestimated (Table 9).

Table 9. *Model performance metrics for NO_2 and PM_{10} predicted concentration levels in Bucharest (Romania) during warm period 2022, when compared with measurements from the National Air Quality Monitoring Network (May-August)*

Pollutant	**Observed mean concentration**	**Modeled mean concentration**	**Root Mean Square Error** (RMSE)	**Correlation Coefficient** (r2)
NO_2 (ppb)	12.58	20.35	8.13	0.66
PM_{10} (µg/m^3)	24.64	18.10	8.59	0.50

3.3 Birmingham Pilot

In BIR, a combination of static and mobile measurements of PM_1, $PM_{2.5}$, PM_{10} were collected using a total of 11 low-cost sensors for 2 months during spring 2023, in the residential area of Selly Oak close to the University of Birmingham with10 seconds time resolution. These measurements were collected using novel instruments of minimal size and weight, which are capable of standalone operation, collection of auxiliary data (e.g. geolocalisation data and meteorology data) and direct connection to the cloud for continuous monitoring and reporting. The data

RI-URBANS (www.RIURBANS.eu) is supported by the European Commission under the Horizon 2020 – Research and Innovation Framework Programme, H2020-GD-2020, Grant Agreement number: 101036245

were collected by members of the staff of the University along with the cooperation of students and members of the local community (i.e. schools and local businesses). These data were complemented with additional measurements of BC, particle number concentrations and Lung Deposited Surface Area from other low-cost sensors also deployed for a limited time period.

3.3.1 Calibration

Calibrations were performed against the research grade instruments located at the Birmingham Air Quality Supersite (two colocation periods, at the start and the end of the campaign). As PM measuring low-cost sensors are known to be affected by the hygroscopic effect resulting from increased RH, tested methodologies from previous campaigns are used for calibration (Bousiotis et al., 2023a). These include estimation of the levels of RH in the local atmosphere (using the data collected by the sensors attached to the instruments) and the correction of the PM values according to them.

3.3.2 Maps

Maps are currently plotted for the measuring period, presenting the PM_1, $PM_{2.5}$, PM_{10} concentration data from both the static and mobile instruments throughout the study area. Furthermore, using statistical methods (Bousiotis et al., 2023b) the contribution of different sources of PM in the area was calculated and will be mapped, potentially showing the evolution and spatial variation of their effect in the study area. Additionally, using the data collected, together with additional data provided by the City Council of Birmingham and applying machine learning methodologies, maps which contain estimates of the PM concentrations throughout the study area in a very dense spatial resolution, even outside the collection time of the mobile instruments, were plotted. The performance of the model has been evaluated with comparison of the modelled data to the data collected from both the static and mobile sensors used during the campaign.

RI-URBANS (www.RIURBANS.eu) is supported by the European Commission under the Horizon 2020 – Research and Innovation Framework Programme, H2020-GD-2020, Grant Agreement number: 101036245

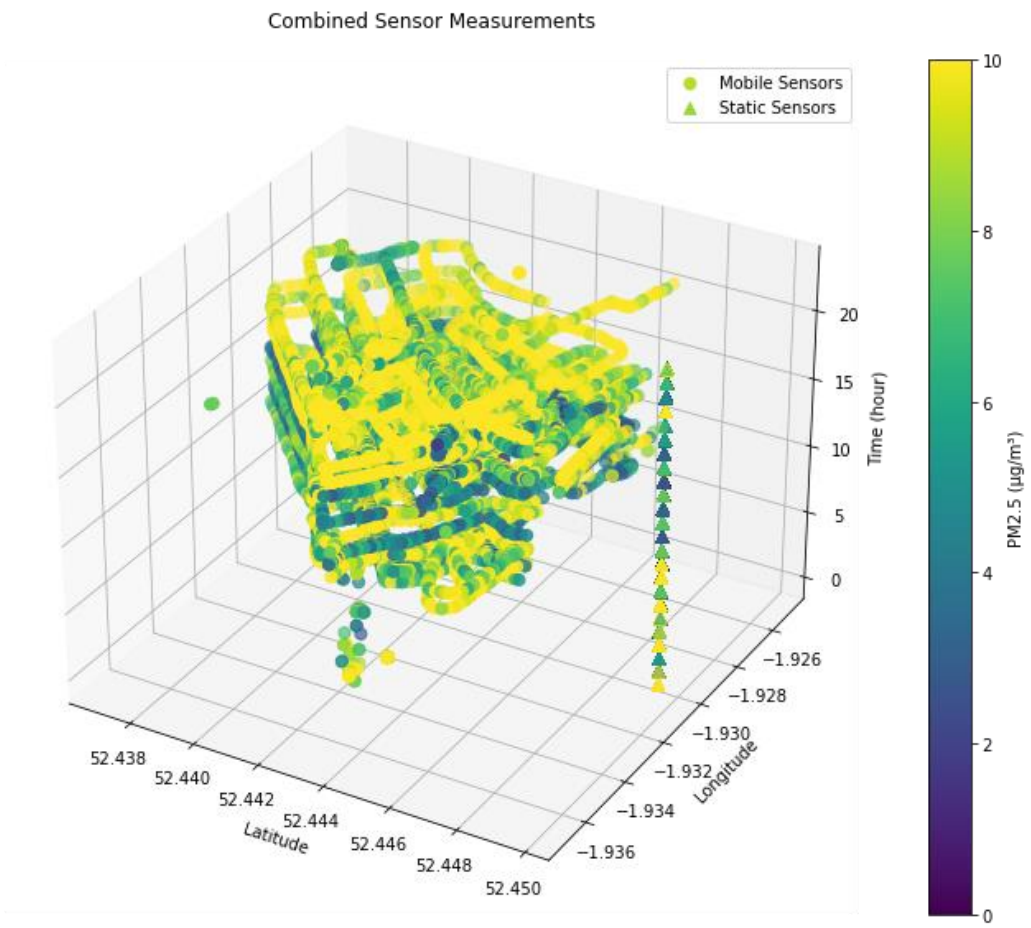

Figure 25. *Three-dimension map (longitude, latitude and time) presenting the estimated $PM_{2.5}$ in the study area in Birmingham, deriving from the analysis of static measurements from low-cost sensors, meteorological conditions and other data and processed using machine learning techniques.*

RI-URBANS (www.RIURBANS.eu) is supported by the European Commission under the Horizon 2020 – Research and Innovation Framework Programme, H2020-GD-2020, Grant Agreement number: 101036245

4. References

Bousiotis, D., Alconcel, L.N.S., *et al.* (2023a) 'Monitoring and apportioning sources of indoor air quality using low-cost particulate matter sensors', *Environment International*, 174(March), p. 107907. Available at: https://doi.org/10.1016/j.envint.2023.107907.

Bousiotis, D., Allison, G., *et al.* (2023b) 'Towards comprehensive air quality management using low-cost sensors for pollution source apportionment', *npj Climate and Atmospheric Science*, 6(1). Available at: https://doi.org/10.1038/s41612-023-00424-0.

CERC. 2021. EMIT Atmospheric Emissions Inventory Toolkit User Guide. Available at: http://www.cerc.co.uk/environmental-software/assets/data/doc_userguides/CERC_EMIT3.4_UserGuide.pdf

Kerckhoffs J, Khan J, Hoek G, Yuan Z, Ellermann T, Hertel O, Ketzel M, Solvang Jensen S, Meliefste K, and Vermeulen R. (2022). Mixed-Effects Modeling Framework for Amsterdam and Copenhagen for Outdoor NO_2 Concentrations Using Measurements Sampled with Google Street View Cars, Environmental Science & Technology 2022 56 (11), 7174-7184, https://doi.org/10.1021/acs.est.1c05806

Kim, Y., Lugon, L., Maison, A., Sarica, T., Roustan, Y., Valari, M., Zhang, Y., André, M., and Sartelet, K.: MUNICH v2.0: a street-network model coupled with SSH-aerosol (v1.2) for multi-pollutant modelling, Geosci. Model Dev., 15, 7371–7396, https://doi.org/10.5194/gmd-15-7371-2022, 2022.

Lugon L., Kim Y., Vigneron J., Chrétien O., André M., André J.-M., Moukhtar S., Redaelli M., Sartelet K. (2022), Effect of vehicle fleet composition and mobility on outdoor population exposure: A street resolution analysis in Paris. Atmospheric Pollution Research, 13, 5, 101365, doi: 10.1016/j.apr.2022.101365.

Ma, X., Longley, I., Salmond, J. et al. (2020) Front. Environ. Sci. Eng. 14, 44. https://doi.org/10.1007/s11783-020-1221-5

Menut, L., Bessagnet, B., Briant, R., Cholakian, A., Couvidat, F., Mailler, S., Pennel, R., Siour, G., Tuccella, P., Turquety, S., and Valari, M. (2021). The chimere v2020r1 online chemistry-transport model. Geosci. Model Dev., 14(11):6781–6811, https://doi.org/10.5194/gmd-14-6781-2021

Ramacher MOP, Kakouri A, Speyer O, Feldner J, Karl M, Timmermans R, Denier van der Gon H, Kuenen J, Gerasopoulos E, Athanasopoulou E. The UrbEm Hybrid Method to Derive High-Resolution Emissions for City-Scale Air Quality Modeling. Atmosphere. 2021; 12(11):1404. https://doi.org/10.3390/atmos12111404

Sartelet K., Couvidat F., Wang Z., Flageul C., Kim Y. (2020), SSH-Aerosol v1.1: A Modular Box Model to Simulate the Evolution of Primary and Secondary Aerosols. Atmosphere, 2020, 11, 525, https://doi.org/10.3390/atmos11050525.

Sartelet, K., Kim, Y., Couvidat, F., Merkel, M., Petäjä T., Sciare J. and Wiedensohler, A. (2022), Influence of emission size distribution and nucleation on number concentrations over Greater Paris. Atmos. Chem. Phys., 22, 8579-8596, https://doi.org/10.5194/acp-22-8579-2022.

Savadkoohi M., Pandolfi M., Reche C., Niemi J.V., Mooibroek D., Titos G. et al. (2023) The variability of mass concentrations and source apportionment analysis of equivalent black carbon across urban Europe, Environ. Int., 178, 108081, https://doi.org/10.1016/j.envint.2023.108081.

Schmitz, O. et al. (2019) Sci Data 6, 190035. https://doi.org/10.1038/sdata.2019.35

Stidworthy, A., Jackson, M., Johnson, K., Carruthers, D., & Stocker, J. (2018). Evaluation of local and regional air quality forecasts for London. Int. J. Environ. Pollut., 64(1-3), 178-191.

RI-URBANS (www.RIURBANS.eu) is supported by the European Commission under the Horizon 2020 – Research and Innovation Framework Programme, H2020-GD-2020, Grant Agreement number: 101036245

Zhong, J, Hood, C, Johnson, K, Stocker, J, Handley, H, Wolstencroft, M, Mazzeo, A, Cai, X & Bloss, W J (2021). Using task farming to optimize a street-scale resolution air quality model of the West Midlands (UK). Atmosphere, 12(8), 983.

RI-URBANS (www.RIURBANS.eu) is supported by the European Commission under the Horizon 2020 – Research and Innovation Framework Programme, H2020-GD-2020, Grant Agreement number: 101036245